JGSB JOURNAL OF THE GEOLOGICAL SURVEY OF BRAZIL

Prospectivity maps for polymetallic skarn and orogenic gold mineralization in the Rio Piranhas-Seridó Domain, Borborema Province (NE Brazil): An aid to exploration targeting

Alan Pereira da Costa[1,2*], Rogerio Cavalcante[1], Nitzschia Regina Rodrigues Domingos[1], Raul Eigenheer Meloni[3], Eduardo Duarte Marques[4], Guilherme Ferreira da Silva[5], Marcos Antonio Leite do Nascimento[2], Poliana Iara de Freitas Toledo[6], Hismana Carjoa Freitas Camara[1]

[1]Serviço Geológico do Brasil - CPRM SUREG-RE/ NANA - Av. Alm. Alexandrino de Alencar, 1402 - Tirol, Natal - RN, 59015-350.
[2] Departamento de Geologia da Universidade Federal do Rio Grande do Norte e Pós-Graduação em Geodinâmica e Geofísica - Campus Universitário - R. das Engenharias, s/n - Lagoa Nova, Natal - RN, 59078-970.
[3] Serviço Geológico do Brasil – CPRM SUREG-SP - Rua Costa, 55 - Cerqueira César, São Paulo - SP - Brasil - CEP: 01304-010.
[4]Serviço Geológico do Brasil – CPRM SUREG-BH – Av. Brasil, 1731, Funcionários, Belo Horizonte - MG - Brasil - CEP: 30140-002.
[5] Serviço Geológico do Brasil – CPRM SEDE-DF - Setor Bancário Norte - SBN Quadra 02, Bloco H - Asa Norte, Edifício Central Brasília, Brasília - DF - Brasil - CEP: 70040-904.
[6] Departamento de Geologia da Universidade do Rio Grande do Norte - Campus Universitário - R. das Engenharias, s/n - Lagoa Nova, Natal - RN, 59078-970.

Abstract

In this study, predictive mineral prospectivity modelling (MPM) was applied to the Bodó, Serra da Umburana, Currais Novos–Santa Luzia, and Caicó–São Fernando–Jucurutu areas of the Seridó Mineral Province, Borborema Province, Northeast Brazil. The MPM was designed to target tungsten (W), molybdenum (Mo), gold (Au), and copper (Cu) mineralization associated with structurally controlled polymetallic skarn and orogenic gold deposits. The predictive models were developed through the integration of geological, geochemical, and geophysical data using the Multiclass Index Overlay (MIO) methodology. Thematic maps with different prospectivity ranges were generated and validated through cumulative curves relating predictive indices to the spatial distribution of the known mineral occurrences. The results demonstrated high model efficiency, with 62% to 88% of the occurrences concentrated in areas of high to very high prospectivity, representing 5% to 25% of the total area of each map. The high prospectivity areas include both known mineralized trends as well as areas yet to be investigated. As such, our MPM results not only confirm the potential of the known mining districts but also present new research and exploration frontiers. Geochemical signatures extracted through factor analysis (FA) revealed robust multielement patterns that support the skarn-type mineralization models. Mineralogical and lithogeochemical data from samples of mineralized zones and/or panned concentrates from prospective targets reinforce the polymetallic nature (W-Mo-Au-Cu) typical of skarn deposits in the study areas. Based on the results obtained from the validation of the prospectivity models, it is concluded that the integrated, mineral systems-based approach is effective in guiding mineral exploration in geologically complex terrain. The predictive maps constitute strategic tools that help reduce uncertainty associated with exploration targeting and attract investment to the region, which is timely given the growing global demand for critical metals.

Article Information

Publication type: Research Papers
Received 22 August 2025
Accepted 9 January 2026
Online pub. 14 January 2026
Editor: Carlos G. Asato

Keywords:
Seridó Mineral Province
Polymetallic skarn
Orogenic Gold
Prospectivity Mapping
Mineral Systems

*Corresponding author
A. P. Costa
E-mail address: alan.costa@sgb.gov.br

1. Introduction

This study presents the results of applying mineral prospectivity mapping (MPM) to polymetallic skarn mineralization (W–Mo–Cu–Au) and orogenic gold systems in the northern segment of the Borborema Province, particularly within the Seridó Mineral Province (SMP) (Figure 1). The research employs updated prospecting techniques in a traditionally mining-oriented region where predictive approaches have been seldom applied. The adopted model integrates the skarn system concepts of Meinert et al. (2005) and the orogenic gold framework of Groves (1993), which provide the theoretical basis for the mappable criteria used in the MPM workflow. To date, no study has systematically applied MPM to W–Mo–Cu–Au skarn systems or orogenic gold mineralization in the SMP, revealing a significant knowledge gap regarding the spatial distribution of these mineral systems.

The use of predictive prospectivity maps based on the mineral systems concept has been increasingly established in recent years as a powerful tool in modern mineral exploration

ISSN: 2595-1939
https://doi.org/10.29396/jgsb.2026.v9.n1.4
Open access at https://jgsb.sgb.gov.br

(e.g. Campos et al. 2017; Boadi et al. 2022; Martins et al. 2022). This approach allows for a significant reduction of the areas to be prioritized for investigation, optimizing the identification of regions with the highest prospectivity and consequently minimizing exploration costs, especially when combined with a solid database of field geological data and an in-depth understanding of the active mineral systems.

The practical relevance of this type of product is exemplified by the lithium favorability map produced by Almeida et al. (2022), whose publication was followed by a marked increase in exploration requests submitted to the Sigmine system (ANM 2025) in the states of Rio Grande do Norte and Paraíba. Although several factors may have contributed to this growth, approximately 80% of the new requests spatially coincide with the map area, indicating that prospectivity products can directly influence mineral exploration dynamics.

In the Brazilian metallogenic context, the Seridó Mineral Province (PMS) stands out as one of the main polymetallic provinces in the country, harboring important deposits and occurrences of tungsten (W) — the largest in South America — and molybdenum (Mo), both associated with skarns; gold (Au), occurring in both skarn-related and orogenic systems; iron (Fe) deposits, in banded iron formations (BIFs); as well as tantalum (Ta) and niobium (Nb), linked to pegmatitic rocks, as reported by Lima et al. (1980), Souza Neto et al. (2008), Cavalcanti Neto (2008), Cavalcante et al. (2015, 2016, 2018), Corrêa (2019a, b), Costa and Dantas (2018) and Costa et al. (2021, 2023a). The mineralizations in this region show strong structural control, characterized by shear zones and fold axes, highlighting the significant interaction between Neoproterozoic-Cambrian tectonothermal events and the genesis of these mineral deposits.

Although the main discoveries of mineral deposits in this province date back to the mid-20th century, much of this knowledge was obtained through conventional prospecting methods, with limited integration of modern approaches. This gap highlights the need for the application of more advanced prospectivity techniques, such as predictive modeling (e.g., Weight-of-Evidence, Index Overlay, Machine Learning), which allow the integration of geology, geophysics, geochemistry, and structural data into predictive models, thereby increasing the robustness of predictions and refining existing geological and metallogenetic models. In this context, the present study contributes by employing updated exploration methodologies through the generation of prospectivity maps based on the Multiclass Index Overlay (MIO) methodology (Carranza 2009), producing information that improves the understanding of the genesis and distribution of the province's mineral deposits. Furthermore, the results provide technical support to guide new research and optimize the exploration of important elements such as W, Mo, Au, and Cu, addressing the growing global demand for these resources.

The main objective was to identify potential areas for polymetallic skarn (W, Mo, Cu, Au) and orogenic gold mineralization, through the generation of prospectivity maps. To this end, the Geological Survey of Brazil (GSB), within the geology and mineral potential of the Borborema Province project, delineated four target areas that encompass the main W and Au deposits and occurrences of the Seridó Mineral Province. This subdivision was adopted because each sector presents distinct geological and metallogenic attributes, which would make it difficult to build a unified prospectivity model capable of accurately representing the entire province. Thus, the segmentation of the areas aims to increase the reliability and spatial resolution of the models, ensuring that the specific geological controls and metallogenic signatures of each area are duly considered.

2. Geology and Mineral Resources

The four areas of the present study are located within the Rio Piranhas–Seridó Domain (PSD), a segment of the Borborema Province in Northeast Brazil (Figure 1). This province is characterized by a complex arrangement of tectonostratigraphic terrains, bounded by shear zones and structured by multiple deformational, metamorphic, and magmatic events related to the collision between the São Francisco Craton and other continental masses during the Brasiliano Orogeny (Almeida et al. 1981; Brito Neves et al. 2000; Van Schmus et al. 2011).

The PSD predominantly consists of crystalline basement rocks with ages ranging from the Siderian to the Orosirian (Medeiros et al. 2021; Costa et al. 2021), in addition to Archean blocks (Oliveira et al. 2013; Costa et al. 2018; Costa et al. 2023a; Santos et al. 2023). This basement is overlain by Neoproterozoic metasedimentary sequences of the Seridó Group, composed of the Jucurutu, Equador, and Seridó formations.

The tectonic evolution of the area reveals at least two orogenic episodes, followed by late- to post-orogenic erosional processes that gave rise to sedimentary basins. The first orogeny, of Riachian age and possibly correlated with the Transamazonian Orogeny, is associated with the joint evolution of the Borborema Province and the Benino-Nigerian Shield, characterizing an accretionary-collisional phase during which the cores of the Caicó and São José do Campestre blocks were amalgamated. This event preceded the formation of the Seridó Basin, composed of rocks intensely deformed and metamorphosed during the second orogeny, of Neoproterozoic age, correlated with the Brasiliano Cycle (Jardim de Sá et al. 1986; Jardim de Sá 1994; Van Schmus et al. 1997, 2003; Medeiros et al. 2021). The Brasiliano Orogeny occurred between 650 and 540 Ma, with a metamorphic peak estimated at 555 Ma, and was marked by the activity of transcurrent shear zones and the intrusion of voluminous Ediacaran plutonism, spatially associated with these structures (Figure 1).

From a metallogenic perspective, the selected areas display a high polymetallic potential, as highlighted in the introductory section. The mineral resources are distributed among active and inactive mines, artisanal mineral extraction, and small deposits (Figure 2), as described by several authors in the regional literature (Luiz-Silva 2000; Trindade 2000; Cavalcanti Neto 2008; Cavalcante et al. 2016; Pereira et al. 2019; Costa et al. 2023a). A synthetic summary of the main geological and metallogenetic characteristics of the most representative deposits is presented in Table 1.

In general, the genesis of these mineralizations is linked to two classical metallogenetic models widely recognized in the international literature (Figure 3 A, B): (i) the skarn-type model, associated with magmatic–hydrothermal systems responsible for polymetallic W–Mo–Au–Cu mineralizations, commonly related to oxidized felsic intrusions and fluid–carbonate rock interaction processes (Meinert et al. 2005); and (ii) the orogenic gold model, which accounts for the formation of auriferous quartz veins hosted in ductile to

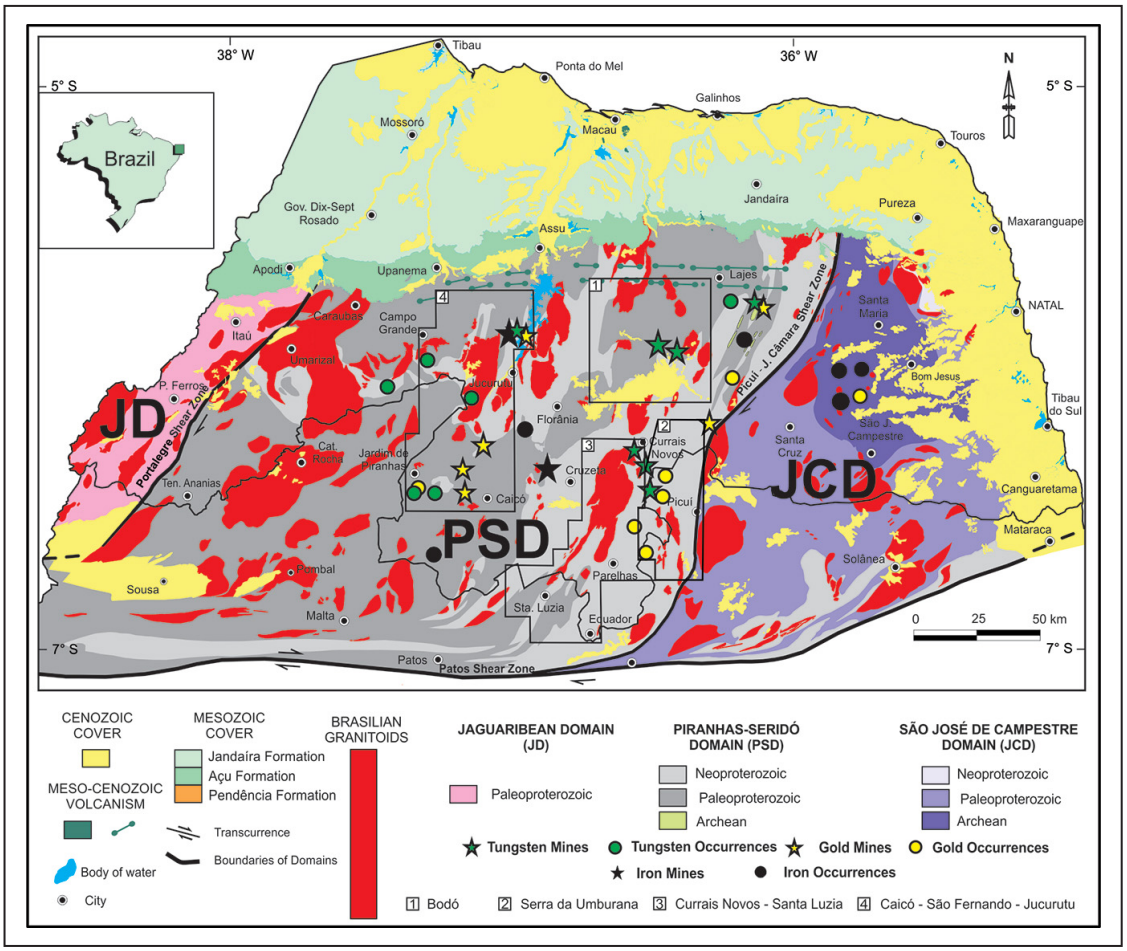

Figure 1: Geological aspects of the northern portion of the Borborema Province (Santos et al. 2023), highlighting the Rio Piranhas-Seridó Domain (PSD) and the polygons representing the study areas: 1) Bodó, 2) Serra da Umburana, 3) Currais Novos–Santa Luzia, and 4) Caicó–São Fernando–Jucurutu (modified from Medeiros 2004; Medeiros et al. 2021).

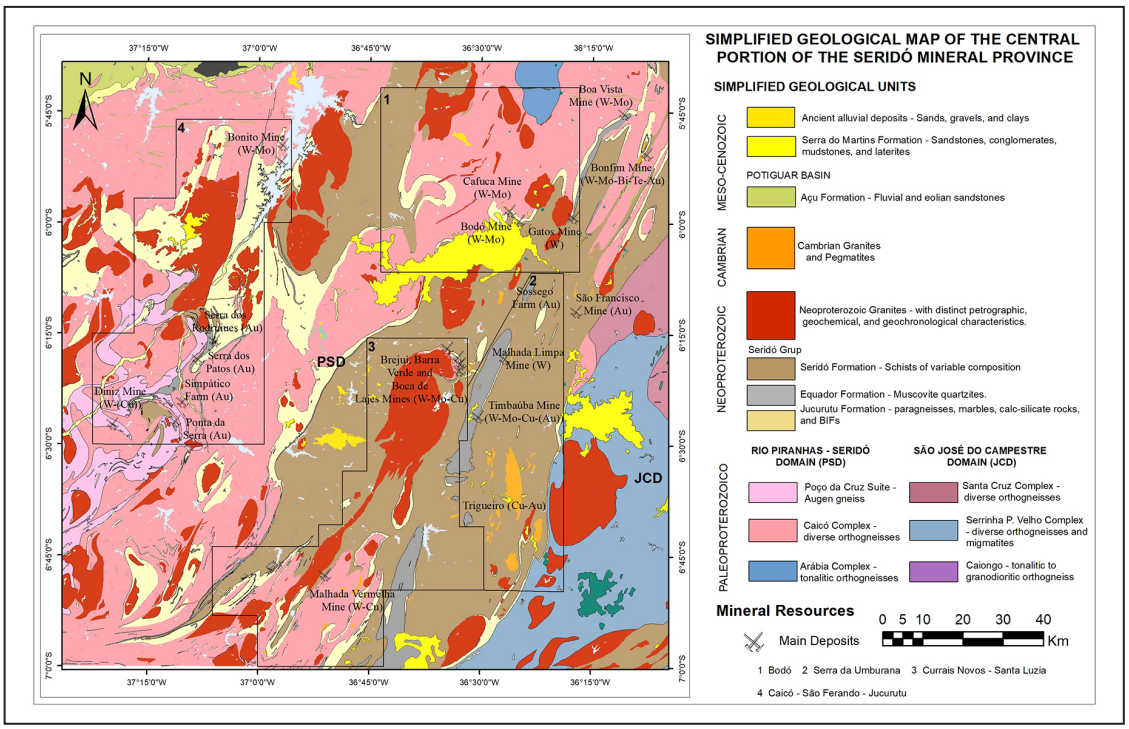

Figure 2: Simplified geological map of the central portion of the Seridó Mineral Province, showing the main lithological units, structural domains, and mineral deposits (Costa et al. 2019).

Table 1: Summary of the main geological and metallogenetic characteristics of the major deposits occurring within the selected areas of the central portion of the Seridó Mineral Province. Data include deposit type, commodity, host unit, average grade, estimated reserves, ore/gangue mineral assemblages, and available geochronological ages. * Pb–Pb model ages in pyrite obtained by LA-ICP-MS (Cunha 2023); ** Re–Os ages in molybdenite after Hollanda et al. (2017); (1) Dantas et al. (2024); (2) Luiz-Silva (2000), (3) Oliveira et al. (2013); (4) Angelim et al. (2006); (5) Torres et al. (1972); (6) Silva et al. (2024).

Deposit	Commodity (Model)	Host Rock / Unit	Grade	Estimated Reserves	Ore / Gangue Minerals	Age (Ma)
São Francisco (Borborema)	Au (Orogenic)	Garnet–biotite–sillimanite schists (Seridó Fm.)	1.1 g/t Au	2.08 Moz Au (1)	Pyrite, chalcopyrite, pyrrhotite, molybdenite, galena	496–500; 504–516 (Pb–Pb)*
Serra dos Rodrigues	Au (Orogenic)	Garnet–sillimanite–staurolite–muscovite–biotite–feldspathic schists (Seridó Fm.)	3.2 g/t Au	105.6 koz Au (2)	Bornite, chalcopyrite, pyrite ± Fe–Ti oxides	–
Serra dos Patos	Au (Orogenic)	Quartzose biotite gneiss and garnet–muscovite–biotite schist (Jucurutu Fm.)	–	–	Bornite, chalcopyrite, pyrite ± Fe–Ti oxides	–
Fazenda Simpático	Au (Orogenic)	Gneisses and muscovite quartzites (Jucurutu/Equador Fms.)	3.0 g/t Au	–	–	–
Ponta da Serra	Au (Orogenic)	Tonalitic to granodioritic orthogneisses (Caicó Complex)	1–3 g/t Au	–	Pyrrhotite, arsenopyrite, pyrite, chalcopyrite, cubanite	–
Bonfim	W–Mo–Au–Bi–Te (Skarn)	Calc-silicate rocks (Jucurutu Fm.)	4.8 wt.% WO_3; 8–40 g/t Au(3)	0.3 Mt; 105 koz Au (4)	Bismuthinite, pyrite, chalcopyrite, pyrrhotite, molybdenite	524 (Re–Os)**
Brejuí – Barra Verde – Boca de Lajes District	W–Mo–(Cu) (Skarn)	Calc-silicate rocks (Jucurutu Fm.)	1.0 wt.% WO_3	11 Mt (6)	Garnet, epidote, calcite, diopside, pyrite, chalcopyrite, molybdenite	554 (Re–Os)**
Malhada Vermelha	W-Cu (Skarn)	Calc-silicate rocks (Jucurutu Fm.)	0.5 1.4%	>2.5Mt (4)	garnet, pyroxene, plagioclase, allanite, apatite, titanite, and scapolite	–
Bodó	W–Mo (Skarn)	Calc-silicate rocks (Jucurutu Fm.)	2.0 wt.% WO_3	9 Mt (6)	Garnet, epidote, diopside, calcite	510 (Re–Os)**
Cafuca	W (Skarn)	Calc-silicate rocks (Jucurutu Fm.)	0.4 wt.% WO_3	0.3 Mt (6)	Garnet, epidote, diopside	–
Diniz	W (Skarn)	Calc-silicate rocks (Caicó Complex)	1.0 wt.% WO_3	–	Pyrite, chalcopyrite	–
Malhada Limpa – Timbaúba	W–(Mo–Cu–Au) (Skarn)	Calc-silicate rocks (Jucurutu Fm.)	0.5 wt.% WO_3	5.5 Mt (6)	Vesuvianite, garnet, diopside, epidote, calcite, pyrite, chalcopyrite, malachite	–
Bonito (Pindoba –Mazagão)	W–Mo (Skarn)	Calc-silicate rocks (Jucurutu Fm.)	0.7 wt.% WO_3	4.0 Mt (3)	Garnet, diopside, epidote, calcite, pyrite	–

brittle–ductile shear zones, resulting from the migration of metamorphic fluids channeled along crustal structures during regional deformation events (Groves 1993).

These models provide the conceptual framework for the interpretation and integration of geological, geophysical, and geochemical data used in the generation of mineral prospectivity maps, grounded in the mineral systems approach (Hagemann and Cassidy 2000; Carranza 2009).

In the Bodó area (Figure 2), W and Mo mineralizations predominate in exoskarns (Figure 4 A and B), with notable mines including Bodó, Cafuca, Umbuzeiro, Queimadas, Saco dos Bois, Gatos, and Riachão. In addition, there are artisanal mines such as Galo, Cinzas, Isidoro, Chupador, Poço dos Cavalos, Porteiras, Casinhas, and Recanto (Cavalcante et al. 2016; Costa et al. 2023a). The mineralizations are structurally controlled, occurring along fold axes, as well as associated with shear zones and pegmatite dikes (specifically in the case of Isidoro). Mineralizations occur predominantly in the metasedimentary rocks of the Seridó Group and, subordinately, in the basement gneisses, along metric-scale shear zones.

The Serra da Umburana area shows potential for W, Mo, Au, Cu, Ta, and Nb mineralization (Cavalcanti Neto 2008; Costa et al. 2023a). Its main mineralizations occur in the Timbaúba and Malhada Limpa deposits, in W-Mo-rich skarns (Torres et al. 1972), with lower levels also mineralized in Cu-Au. The mineralizations are controlled by fold axes and shear zones (Cavalcanti Neto 2008). Similar skarn levels are found in the Pilões, Trigueiro, Alto Ribeira, and Riacho das Corujinhas regions, within a stratigraphic transition context between the metasedimentary rocks of the Jucurutu and Equador formations, associated with faulting at outcrop scale, with Cu and Au occurring in boudins within quartz veins at the

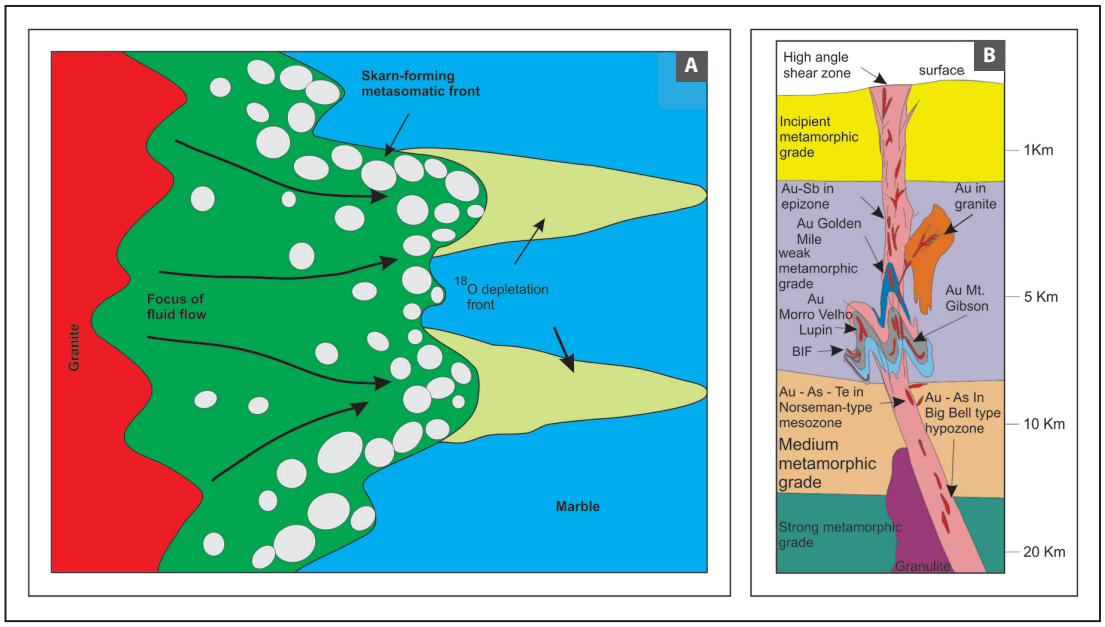

Figure 3: Conceptual models representing the main types of metallic deposits in the Seridó Mineral Province (A) Schematic model of skarn formation showing the metasomatic front developed at the contact between the intrusive granite and the carbonate host rock, emphasizing the fluid flow focus and the ^{18}O-depletion front (Meinert et al. 2005). (B) Genetic model of orogenic gold deposits illustrating the vertical zonation and main styles of auriferous mineralization (with examples) formed along crustal shear zones, from epizonal to deep metamorphic levels (Biondi 2003, adapted from Groves 1993).

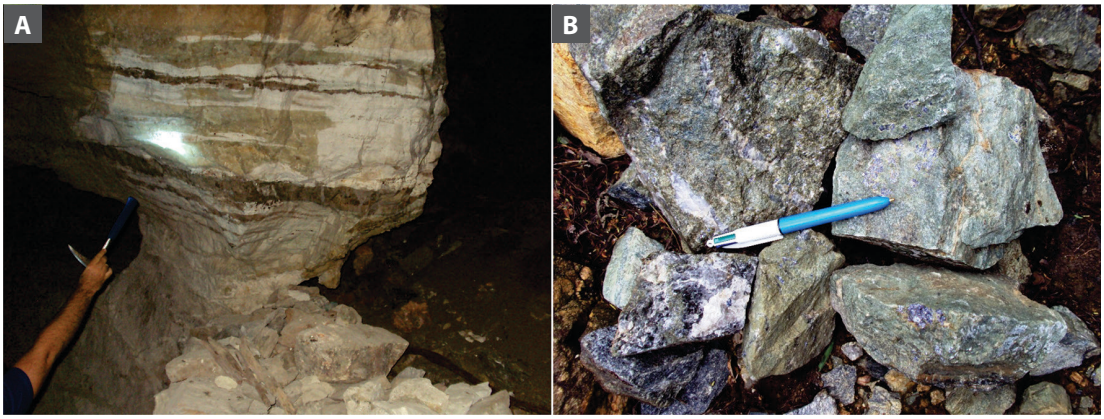

Figure 4: A) Scheelite mining front at the skarn level in the central gallery of the Bodó mine; B) Mineralized skarn blocks with Mo and W at the Galo artisanal mine.

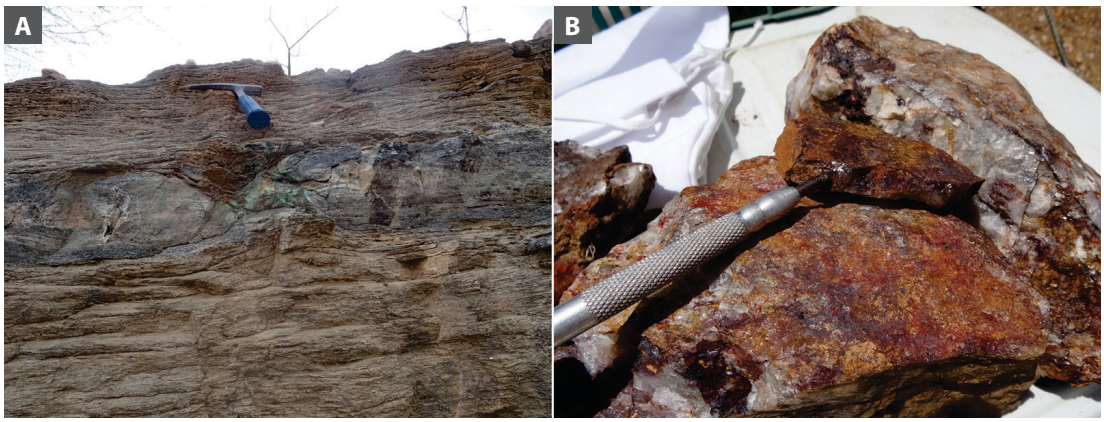

Figure 5: A) Boudinaged quartz veins in calc-silicate rock, with malachite mineralization reaching 6.2% Cu and 1.5 ppm Au – Cipó Site (AP-R-129). B) Sulfide-bearing quartz veins in the tailings of the abandoned Várzea Redonda artisanal mine.

centimeter-scale skarn levels (Figure 5A). In the same area, Au is also associated with quartz veins at Várzea Redonda and Santana localities (Figure 5B).

The Currais Novos–Santa Luzia area stands out for its significant W and Mo mineralizations (Figures 6A and 6B), hosting the largest deposits in South America (W) and in Brazil (Mo) (Costa et al. 2023a), with notable mines including Brejuí, Barra Verde, Boca de Lage, Saco dos Veados, Umbuzeiro, Quixaba, and Porteira. The structural control of mineralizations in the main deposits is associated with fold axes affecting the skarns of the Jucurutu Formation, particularly at the contact with marbles. Cu mineralizations also occur associated with shear zones in the Brejuí and Boca de Lages deposits, as well as in the Acauã artisanal mine. (Cavalcante et al. 2016; Costa et al. 2023a).

The Caicó–São Fernando–Jucurutu area shows potential for W, Au, and Cu mineralizations, which occur both in Neoproterozoic lithotypes of the Seridó Group and in gneisses of the crystalline basement (Luiz-Silva 2000; Costa et al. 2023a). Among the most relevant deposits and prospects are the Bonito and Diniz W deposits, as well as the Água Fria, Angicos, Três Riachos, Retiro, Ferreiro, Lagoa Rachada, Mutamba, and Jacaré artisanal mines, which occasionally contain low grades of Cu, Au, and Mo (Figures 7A and 7B). Au mineralizations occur in the Serra dos Rodrigues, Serra dos Patos, Fazenda Simpático, Ponta da Serra, Anastásio, and Tapera deposits and artisanal mines (Figures 7C and 7D).

3. Materials and methods

The prospectivity maps presented in this study were developed using an integrated approach that combines geological, geophysical (gravimetry, airborne gamma-ray spectrometry, and aeromagnetics), and geochemical (stream-sediment) datasets, processed according to the Multiclass Index Overlay (MIO) methodology of Carranza (2009). Their construction employed both publicly available data provided by the Geological Survey of Brazil (GSB; https://geosgb.sgb.gov.br) and information acquired during field campaigns, which included the collection and updating of lithological and structural data, as well as the processing of prospective geochemical signatures, geophysical anomalies, and remote sensing products. The systematic integration of these datasets enabled the generation of evidence layers and prospectivity models consistent with the mineral systems framework (Figure 8).

The prospectivity models for each area, along with their respective components and weights, were originally organized in descriptive tables presented alongside each thematic map. In this article, this information has been consolidated into Table 2, preserving the particularities of each area. The processing for generating the input data based on mappable criteria produced raster files with values ranging from 0 to 10.

The Multiclass Index Overlay (MIO) methodology (Carranza 2009) employed in this study for integrating the input data is deterministic in nature and based on expert judgment. This approach takes into account prior knowledge of the area, encompassing both existing mineral resources and their geological characteristics, such as structural controls and geochemical associations, as well as features of the mineral system operating in the area. Since it does not involve direct statistical calculations, the assignment of weights is carried out based on previously established qualitative and quantitative criteria. These factors require performing a series of tests and generating different prospectivity models, which are ultimately refined and validated using cumulative curves to determine the most efficient models. In this study, each piece of evidence was assigned a weight proportional to its relative importance in the prospectivity model, according to the degree of knowledge the authors had of the mapped areas, and is subject to differing interpretations.

The choice of the MIO methodology is justified by its flexibility and robustness in heterogeneous geological contexts and in datasets with variable coverage and resolution, allowing the weighted integration of multiple criteria derived from both mappable evidence and theoretical parameters of the mineral system. During the generation of evidence maps, weights greater than 1 were assigned to the criteria considered most significant (Table 2). For the Caicó–São Fernando–Jucurutu and Currais Novos–Santa Luzia maps, weights of 10 were applied to the prospective geochemical halo and gamma-ray spectrometry data to normalize their original values (0–1) to the same scale used for the other input datasets (0–10), ensuring compatibility among all parameters used in the model.

The integration of geological, geophysical, structural, and geochemical datasets was guided by the different components of the mineral systems framework (Figure 8) and by the conceptual deposit models represented in the studied areas (Figure 3), considering the expected role of each criterion in the processes of mineral generation, migration, and deposition. Accordingly, the weights applied to the evidence

Figure 6: (A) Skarn level mineralized in W at the contact with the marbles of the Jucurutu Formation at the Brejuí Mine. B) Skarn sample mineralized with molybdenite at the Brejuí Mine (Currais Novos-RN).

Figure 7: (A) Outcrop in an abandoned excavation pit of the Bonito W and Mo mine (Jucurutu – RN, AP-008); B) Main pit and entrance to the underground gallery of the Diniz W mine, with mineralization controlled by a shear zone hosted in gneisses of the Caicó complex basement, with metric width and vertical orientation (Serra Negra do Norte, AP-172); C) Serra dos Patos Au artisanal mine (São Fernando – RN, AL-069), Au mineralization in quartz veins associated with schists of the Seridó Formation; D) Au artisanal pit hosted in quartz veins within a shear zone in the gneisses of the Caicó Complex (Faz. Ponta da Serra, Caicó – RN, AP-030).

and prospectivity maps represent the potential contribution of each element to the mineralizing processes, as defined by the adopted mineral system model.

The sources of metalliferous fluids were inferred through two complementary approaches: (i) the identification of granitic rocks exposed at the surface or inferred from gravimetric anomalies, representing potential sub-outcropping bodies associated with magmatic fluid release; and (ii) the recognition of geological units described in the regional literature as potential sources of such fluids (Luiz-Silva 2000; Lucas et al. 2024).

The intense granite magmatism that characterizes the Seridó Mineral Province is interpreted as the main thermal mechanism capable of driving the circulation and migration of mineralizing solutions through multiple crustal levels. The distinction between outcropping and sub-outcropping granites reflects variations in crustal depth, the degree of preservation of lithostratigraphic units, and the availability of lithotypes favorable to replacement and mineral precipitation processes, both in proximal and distal settings.

The data used in this study, as well as the treatments applied at each stage, are described below.

3.1 Geological data

The geological data used in this study consisted of layers of lithologies, structures, and mineral resources, obtained from the 1:100,000 scale cartographic databases of the Geological Survey of Brazil (GSB) or interpreted from satellite images. These data were consolidated during five fieldwork campaigns, totaling approximately 100 days, which included the collection of rock samples from mineralized zones and host rocks of the main deposits, artisanal mines, and mineral occurrences, stream sediment and pan concentrate sampling to check for Au geochemical anomalies, and the construction of schematic geological profiles to update the cartographic bases to be used in the maps. These data were processed using ArcGIS 10.8.2 with the Spatial Analyst module to generate raster files integrating the evidence maps. Lithology provided information for the components of fluid sources, metals and ligands, energy sources, and lithostratigraphic units. Structural layers contributed to the items of fluid migration conduits and deposition gradients. Mineral resource data were used in the final stage of the study as control points for validating the generated models, through the comparison between index and prospectivity values, and their respective percentages within the mapped areas where mineral resources occur, presented in the form of cumulative response curves.

3.2 Geophysical data

The geophysical dataset is composed of airborne magnetometry and gamma-ray spectrometry data from the Paraíba – Rio Grande do Norte Aerogeophysical Project (CPRM 2010), as well as terrestrial gravity data acquired by the BSG within the ARIM Seridó Project (Costa et al. 2023a).

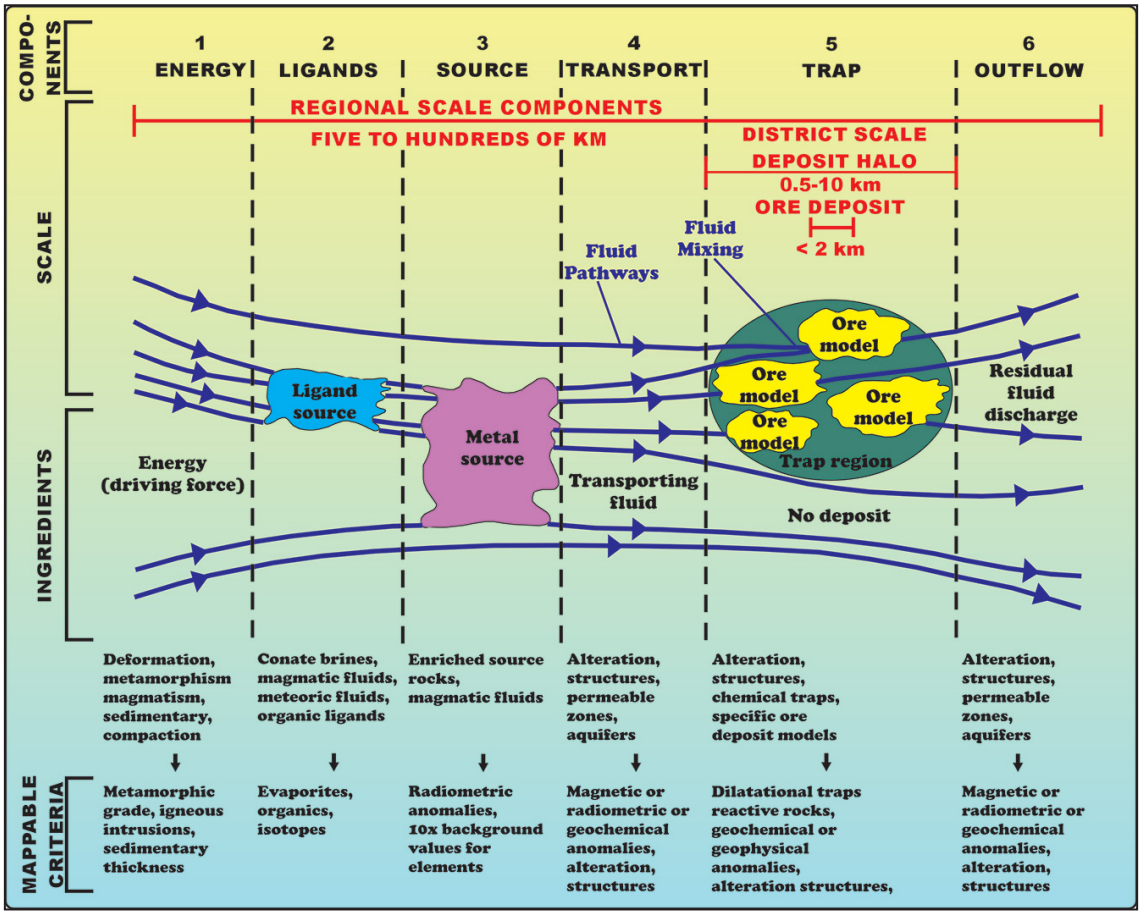

Figure 8: Mechanisms of mineral deposit formation from the perspective of mineral systems (Hagemann and Cassidy 2000).

Pre-existing gravity data obtained by various research institutions were also incorporated and later compiled by Oliveira (2008) into a unified database.

The airborne survey was carried out with flight lines spaced 500 m apart and an average height of 100 m above the ground. The cesium vapor magnetometer (0.001 nT sensitivity) acquired data with a resolution of approximately 8 m, and the gamma-ray spectrometric system with sodium iodide crystals performed measurements at intervals of approximately 80 m, varying according to the aircraft's speed. Gravity data are collected at variable intervals, between 2 km and 10 km, depending on the acquisition project. In the study area, the 2 km grid predominated, with data acquisition primarily performed using the CG-5 Autograv gravimeter (Scintrex), which has a reading resolution of 0.001 mGal. The geophysical data were processed to represent the geological processes of the mineral system, using the Oasis Montaj (v. 9.10) and ArcMap (v. 10.8.2) software. Aerogeophysical data were interpolated upon grids with a spacing of 125 m for magnetometry (bidirectional interpolation method) and gamma-ray spectrometry (minimum curvature method), and 5 km for gravity (minimum curvature method). From the gravity data, the free-air and Bouguer anomalies (density of 2.67 g/cm³ for topographic correction) were calculated. The residual component of the Bouguer anomaly (> 50 km) was obtained with a Gaussian filter after analysis of the power spectrum (Spector and Grant 1970). Upward continuation at different depths was also applied to attenuate shallow signals and enhance deep responses, and tilt angle (Miller and Singh 1994) was applied to residual anomalies—continuous or not—to highlight possible granitic bodies, outcropping or subsurface, associated with negative density contrasts. The magnetic anomaly was corrected by IGRF (International Geomagnetic Reference Field) and the following transformations and filters were applied: reduced-to-the-pole, matched filter (regional and residual separation, upward continuation, tilt angle and first vertical derivative), to highlight lineaments associated with the migration of mineralizing fluids. Relational parameters between K, eTh, and eU were used to highlight geological processes. The anomalous eU (Saunders et al. 1993) highlighted hydrothermal processes related to uranium enrichment, while the eU/eTh ratio indicated uranium mobilization and increased silica. The eTh/K ratio and the F factor mapped potassium alterations associated with hydrothermal zones.

3.3 Geochemical prospectivity data

The geochemical layers used in the four prospectivity maps were based on the factor analysis (FA) results using stream sediment geochemical data. This analysis aims to identify the principal geochemical associations related to skarn mineralization in the studied area, which are represented in each extracted factor. FA is a highly robust method for achieving this objective, as it provides the most accurate correlation structure among variables compared to other multivariate techniques (Reimann et al. 2002).

Table 2: Integrated table of theoretical criteria, mappable criteria, and input data within the context of Mineral Systems for the prospectivity maps of the areas (BD – Bodó, CS – Currais Novos – Santa Luzia, SU – Serra da Umburana, and CSJ – Caicó – São Fernando – Jucurutu).

Mineral System Components	Theoretical Criterion	Mappable Criterion	Input Data	Weights in the evidence maps				Weights in the prospectivity maps			
				BD	CS	SU	CSJ	BD	CS	SU	CSJ
Fluid Source	Heat source distance	Negative Bouguer anomaly – Granitic bodies	Euclidean distances <1000 m, upward continuation at 500 m and 1000 m. Negative anomalies converted to positive	1	1	5	1	2	2	1	4
	Skarn generation	Jucurutu Formation, Seridó Formation, Caicó Complex	Reclassified unit shapefile	1	1	1	1				
Energy Source	Granite magmatism	Outcropping granites	Shapefile of reclassified granite-pegmatite lithologies	1	1	1	1	2	1	1	3
		Suboutcropping granites	Euclidean distances <1000 m, upward continuation at 500 m and 1000 m. Negative anomalies converted to positive	1	2	2	1				
Conduits for fluid migration	Deep Structure	Non-magnetic lineaments	Reduced to the pole and upward continuation at 2000 m	1	1	1	1	1	1	1	2
		Gravity and magnetic lineaments	Euclidean distances <1000 m, upward continuation at 1000 m, 2000 m, and 3800 m. Negative anomalies converted to positive in the case of gravity data	1	1	1	1				
Deposition gradients	Ductile structures	Axes of regional folds	Structures mapped at 1:100,000 scale	1	–	–	–	3	2	5	5
	Shallow Structures	Structural lineaments	Euclidean distances <100 m extracted from satellite images	–	–	1	–				
		Magnetic lineaments interpreted as ductile	Euclidean distances <1000 m derived from magnetic lineaments from the first vertical derivative	–	–	1	–				
		Magnetic lineaments	Euclidean distances <1000 m derived from magnetic lineaments from the first vertical derivative	3	1	1	1				
	Zones with Relevant Geochemical Signatures	Geochemical Halos	Maps with drainage basin centroids – IGPM (W-Cu)	–	–	2	–				
			Maps with drainage basin centroids – IGPM (W-Au)	–	–	2	–				
			Maps with drainage basin centroids – IGPM (Bi-W)	–	–	–	10				
			Maps with drainage basin centroids – IGPM (W-Mo-Cu-Pb-Zn-Sn-Bi-Sb-Te-Ag)	–	1	–	–				
			Maps with drainage basin centroids – IGPM (W-Mo)	1	–	–	–				
		Anomalous Uranium	Anomalous uranium by (linear regression)	–	–	–	10				
		Zones enriched in eU/eTh	eU/eTh	–	–	1	–				
		Hydrothermal alteration	eTh/K	1	10	–	–				
		Potassic alteration	F-Factor = K*(eU/eTh)	1	–	1	–				
Lithostratigraphic Unit	Lithologies with higher probabilities of hosting mineralization	Classified geological map	Reclassified lithology shapefile	1	1	1	1	3	3	3	4

Before applying the FA, the geochemical data were assessed for some important procedures to ensure acceptable performance. The amount of censored data for each variable considered in FA was < 30% of the total samples, and the concentrations found in lower detection limits (LDL) of the analytical method were replaced by LDL/2. This procedure ensures an enhanced performance of FA, thereby avoiding spurious correlation between the variables. The Shapiro-Wilk test was applied to assess the normality of the variables with raw and log-transformed data. Even after applying data transformation, the variables showed non-normal behavior ($p < 0.05$). This fact confirms that data with a normal distribution are rarely found in geochemical variables, due to the influence of multiple populations (Reimann et al. 2008; Grunsky 2010; Lapworth et al. 2012). Thus, the elements used for the FA model in each prospectivity map were those related to each mineralized area (knowledge-driven procedure) and also validated by the statistical tests applied. Therefore, they are as follows: 1) Serra das Umburanas area (Cu-Au in skarns), W, Bi, Mo, Cu and Cd; 2) Bodó area (W in skarns), W, Bi, Mo, Sn and Nb; 3) Caicó-São Fernando-Jucurutu area (W-Au in skarns), W, Bi, Mo, Cu and Cd; 4) Brejuí-Santa Luzia (also W-Au in skarns), W, Bi, Mo and Zn. It is also worth noting that Au was not used in the FA models due to its low detection rate (resulting in more than 90% of censored data). Nevertheless, the presence of other important elements in the ore paragenesis is sufficient to identify significant mineralization targets in a given area using FA models, as demonstrated by Marques et al. (2023) in their study on the Au mineralization potential of the NW Quadrilátero Ferrífero, Brazil.

After the statistical assessment of the variables, the stream sediment geochemical data were normalized using the isometric log-ratio (ilr) transformation by the compositional data approach, using the ilr-balances (Egozcue et al. 2003). This technique mitigates the closure effect of compositional data (constant sum, 1,000,000 mg/kg = 100%) and reduces the occurrence of spurious correlations, thereby enabling more accurate interpretations of FA results (Pawlowsky-Glahn et al. 2015; Pawlowsky-Glahn and Egozcue 2016). Moreover, this data transformation enhances mineralization signatures, as regional-scale geochemical surveys typically exhibit substantial variation related to lithological diversity and other geological processes, which may obscure the mineralization signal (Carranza 2011; Yousefi et al. 2012). The factor extraction method used was Principal Components, the eigenvector rotation applied was the Varimax, and the Kaiser criterion and the scree plot were used to determine the number of factors to retain (Kaiser 1960). Factor loadings were considered significant when greater than 0.45.

The FA models presented at least one factor with a geochemical signature that indicated important targets for skarn mineralization. 1) The Serra das Umburanas area presented the Bi-W signature; 2) the Bodó area presented the Mo-Sn-W signature; 3) the Caicó-São Fernando-Jucurutu area displayed the Bi-W-Mo signature; and 4) the Currais Novos-Santa Luzia area showed the W-Mo-Bi signature. The elements partitioning (ilr balances) and the factor loadings for each model are presented in the supplementary material (SM 1). Each of the four aforementioned models was employed to derive the "Geochemical Mineralization Prospectivity Index" (GMPI; Yousefi et al. 2012, 2014), which enhances the detection of multielement anomalous signatures. The output of this procedure is considered a key input for generating mineral prospectivity maps based on fuzzy logic (Knox-Robinson 2000; Carranza and Hale 2001; Nykänen et al. 2008; Yousefi et al. 2014; Yousefi and Carranza 2016). Therefore, the factor scores for each sample in the four considered models were "fuzzified" using the following logistic function:

$$\mathrm{GMPI} = \frac{e^{Fe}}{1+e^{Fe}}$$

where "Fe" refers to the factor score for each sample. The resulting modified scores represent the GMPI for each geochemical association linked to mineralization (Yousefi et al. 2012). Figure 9 displays a flowchart summarizing the procedures applied to the geochemical data.

All statistical analyses were performed using Statistica® (StatSoft – version 14), Microsoft Excel, and CoDaPack (version 2.02.21; Comas-Cufí and Thió-Henestrosa 2011). Mapping and geoprocessing were carried out using ArcGIS (version 10.8.1).

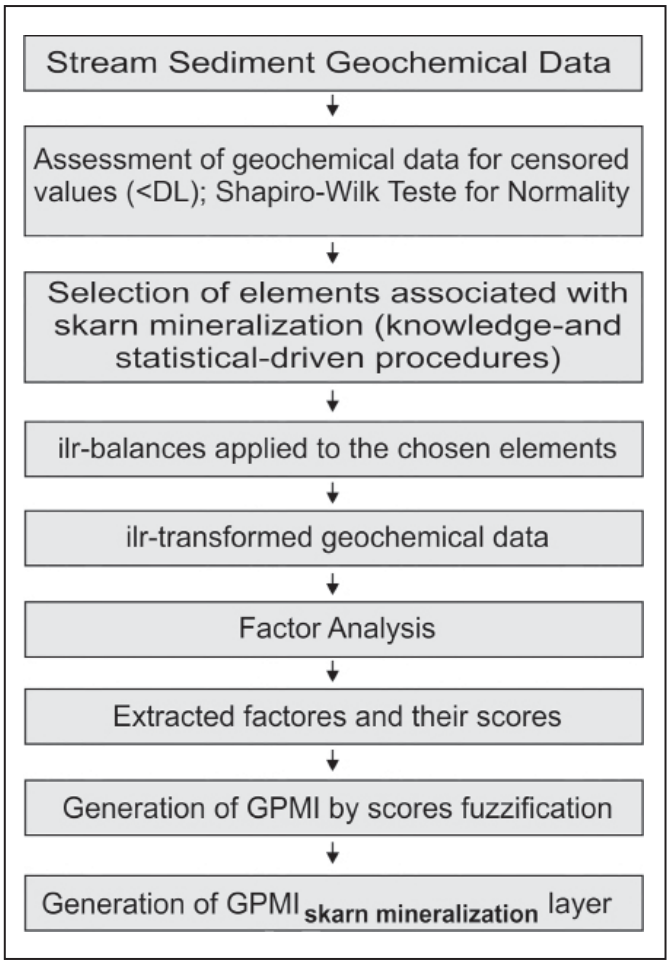

Figure 9: Flowchart summarizing the procedures applied to the geochemical data.

4. Results

4.1 Evidence Maps and Prospectivity Maps

After the initial processing, the datasets were integrated to generate the evidence maps, as illustrated in the flowcharts for each area (Figure 10). The level of knowledge about the data and the degree of certainty of their occurrences were considered in the assignment of their weights. The integration of this information using the same methodology (Multiclass Index Overlay) enabled the generation of predictive models capable of classifying the study areas into different prospectivity classes, defined as low, medium, high, and very high prospectivity index. The values assigned to each class vary according to the specific parameters of each generated map (Figures 11 to 14). The evidence maps are provided as auxiliary insets within each map and are labeled according to the components of the mineral system (Figures 11 to 14).

4.2 Validation of the Prospectivity Models

For the validation of the prospectivity models generated for the areas analyzed in this study, cumulative curves were created relating the final prospectivity indices to the spatial distribution of known occurrences and the percentage of the total mapped area (Figures 15A to D). Models are considered effective when the curves representing the distribution of occurrences (generally steeper) are significantly separated from the curve representing the distribution of the total area. This behavior indicates that the model is capable of prioritizing regions with a higher probability of mineralization, thereby reducing the area to be explored and optimizing resources allocated to mineral exploration. Table 3 correlates the prospectivity potential of each analyzed area with its respective prospectivity indices.

In the Bodó area (Figure 11), model validation indicated that 81.7% of the 82 primary occurrences of W and Mo are located in areas of high and very high potential, which represent 25.23% of the total map area (Figure 15A). In the Serra da Umburana region (Figure 12), model validation revealed that 76.5% of the 17 Cu and Au occurrences coincided with areas classified as having high and very high prospective potential, which account for only 5% of the total map area, as indicated by the validation curves (Figure 15B). In the Currais Novos–Santa Luzia region (Figure 13), model validation based on 66 W occurrences showed that 67.0% of these points are concentrated in areas with medium to very high prospectivity indices, which cover only 10.86% of the total map area, as illustrated in the validation curves (Figure 15C). In the Caicó–São Fernando–Jucurutu area (Figure 14), validation demonstrated that 62% of the 151 W and Au occurrences are located in areas of high and very high potential, which occupy only 23% of the total map area (Figure 15D). These results highlight the good performance of the models, as demonstrated by the validation curves for all areas.

4.3 Lithogeochemical and Mineralogical Data

The results obtained from the analyses of this dataset reinforce the interpretation that these areas possess polymetallic potential and demonstrate the prospective relevance of the zones highlighted in the four maps presented here. In the Bodó and Currais Novos–Santa Luzia areas, mineralized skarn levels in W and Mo were identified, associated with regional fold axes, faults, and shear zones. These occurrences are present in both metasedimentary rocks of the Jucurutu and Seridó Formations and in the crystalline basement of the Caicó Complex. The mentioned geological units and structures coincide with sectors classified as having high to very high prospectivity indices in the respective maps (Figures 11, 13, 16A and B; Table 4).

In the Serra da Umburana area, skarn and amphibolite levels mineralized in Cu, Au, bismuth, and tellurium (Te) are observed in various outcrops in the Trigueiro and Sítio Cipó regions, located in the southwestern portion of the map, in areas with high to very high prospectivity indices (Figures 12 and 16C). Mineralizations of these elements are already known on the eastern flank of Serra da Umburana with the Timbaúba and Malhada Limpa deposits (Cavalcanti Neto 2008). Furthermore, free Au fragments were identified in stream sediments and Au panning concentrates in the Várzea Redonda and Fazenda Sossego localities (Figures 16D, Table 4).

In the Caicó–São Fernando–Jucurutu area, W and Au mineralizations are associated with shear zones with metric widths and lengths ranging from a few hundred meters, reaching up to two kilometers. These structures cut through Paleoproterozoic rocks of the Caicó Complex and Neoproterozoic rocks of the Seridó Group, controlling the occurrence of W and Au mineralizations in the regional rocks, as observed in the Diniz, Ferreiro, Reforma, Três Riachos, and Lagoa Rachada sites for W (Figures 14, 16 E and 17), while Au mineralizations are observed in the Serra dos Patos, Serra dos Rodrigues, Fazenda Simpático, Ponta de Serra, Tapera, Anastásio, and Fazenda Cachoeira localities (Figures 14 and 16F, Table 4).

At the Diniz deposit, in addition to scheelite mineralization, millimeter-scale faults filled with copper sulfides (chalcopyrite) are observed in the orthogneisses enclosing the mineralization (Figures 16G and H). Mineralogical and lithogeochemical analyses of ore concentrates collected at the beneficiation plant indicated the presence of Au in low concentrations associated with the mineralization of this deposit (Figure 16I, Table 4). The main mineralizations in this area occur in regions with high to very high prospectivity indices, according to the generated model (Figure 14). The model also proved sensitive to other types of mineralizations, such as Ba, Mo, and Cu, reinforcing the activity of magmatic–hydrothermal systems in the region. Skarn-type deposits in more traditional models occurring in other localities of Seridó, such as the Bonito Mine (W), were also correctly mapped, confirming the robustness and applicability of the methodology (Figure 14).

5. Discussions

The predictive models developed for the areas analyzed in this study were designed considering the evolution of structurally controlled magmatic-hydrothermal systems in the genesis of W-Mo, Au, and Cu mineralizations, which affect both the crystalline basement rocks (Caicó Complex) and the Neoproterozoic metasupracrustal cover rocks of the Seridó Group in polymetallic skarns and orogenic gold models (Figure 18). Their design take into account the presence of non-outcropping or sub-outcropping granitic intrusions, interpreted through negative gravity anomalies observed in

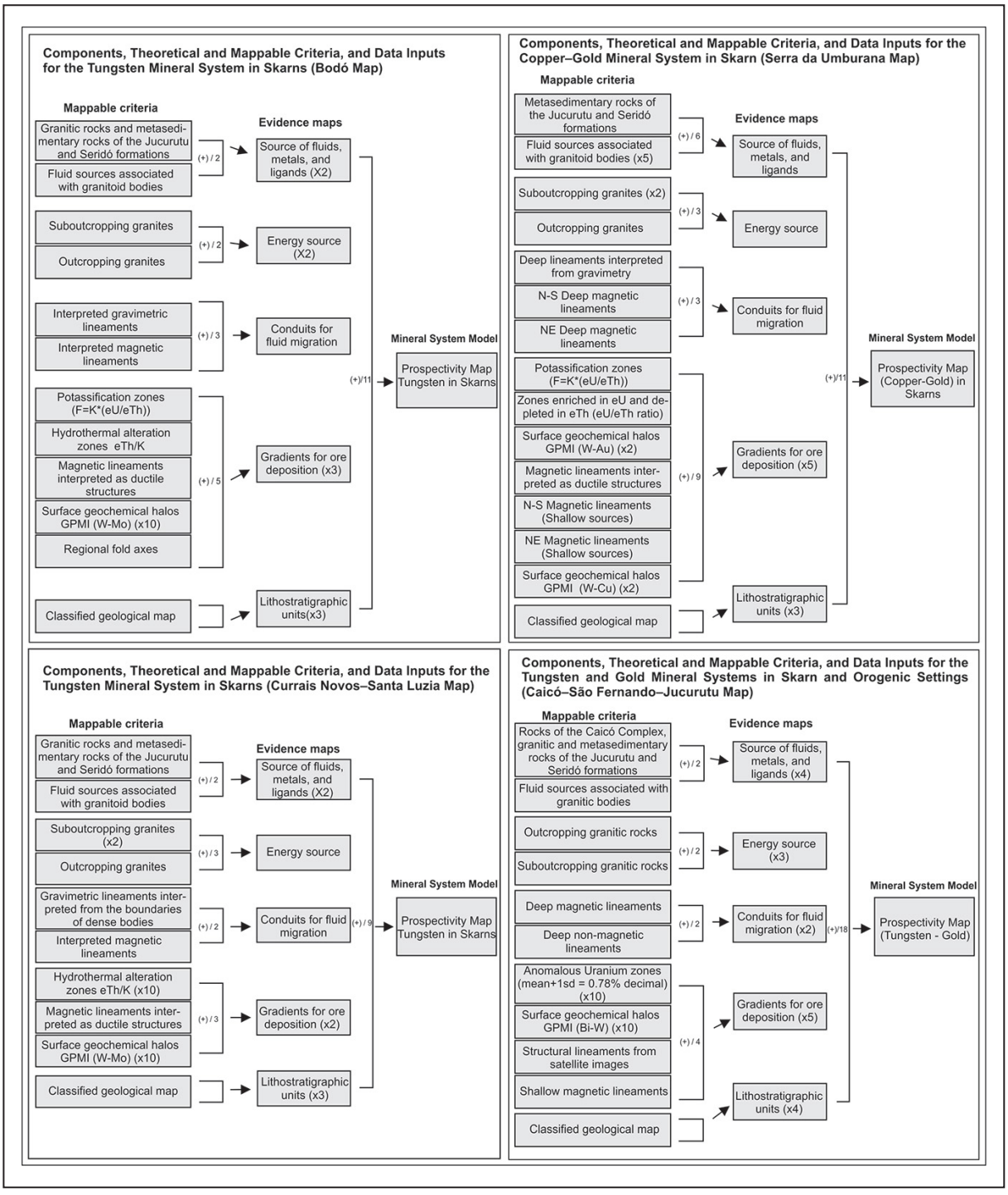

Figure 10: Flowchart of the data equation used for generating the evidence maps and the mineral system model for the four study areas. Multiplication factors (x) were applied to the most important mappable criteria with the highest degree of knowledge, and then summed (+). The value obtained from the sum was divided (/n) by the number of mappable criteria in each component of the equation.

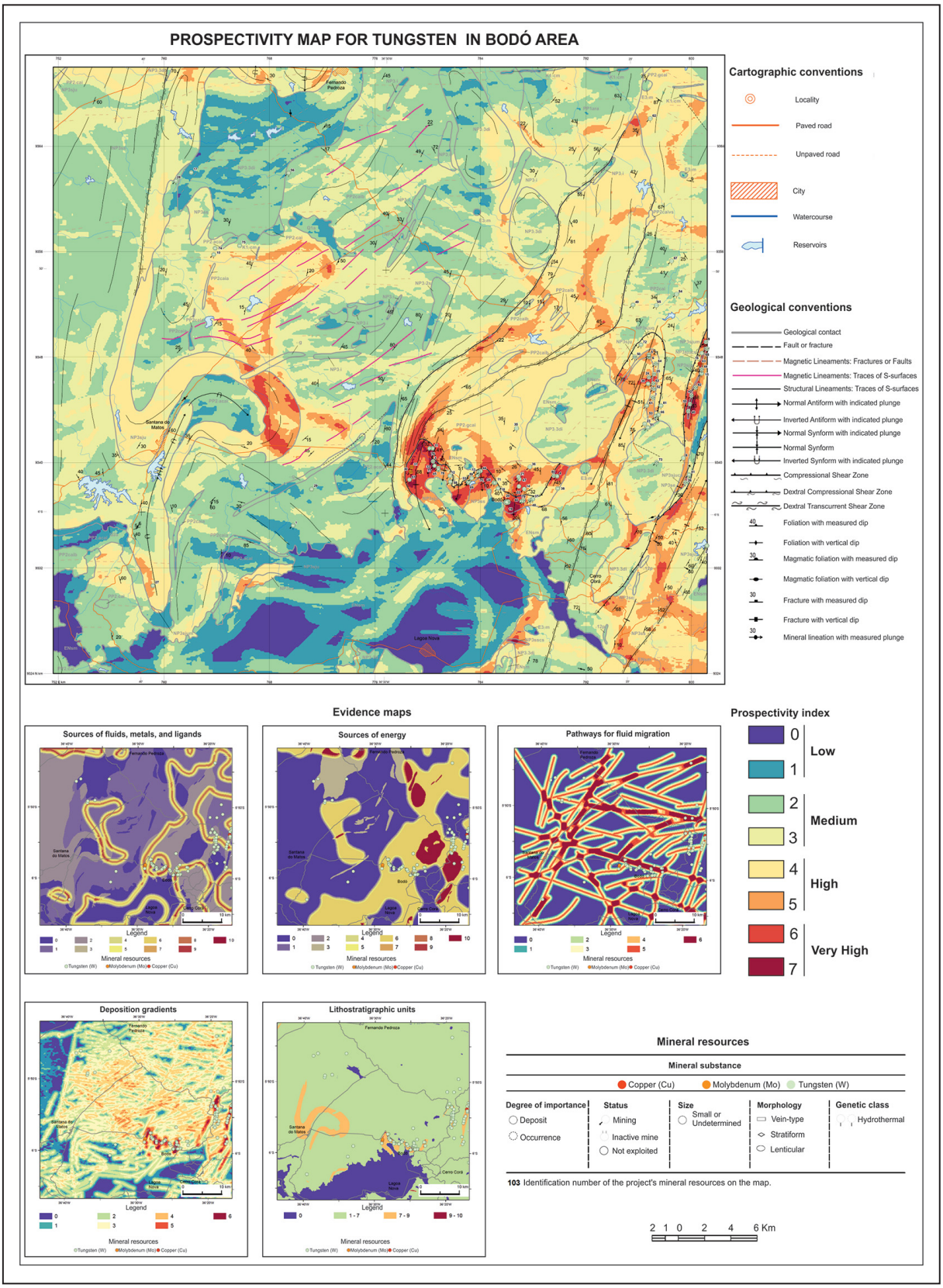

Figure 11: Simplified prospectivity map with its evidence maps for W in the Bodó area (Adapted from Cavalcante et al. 2024).

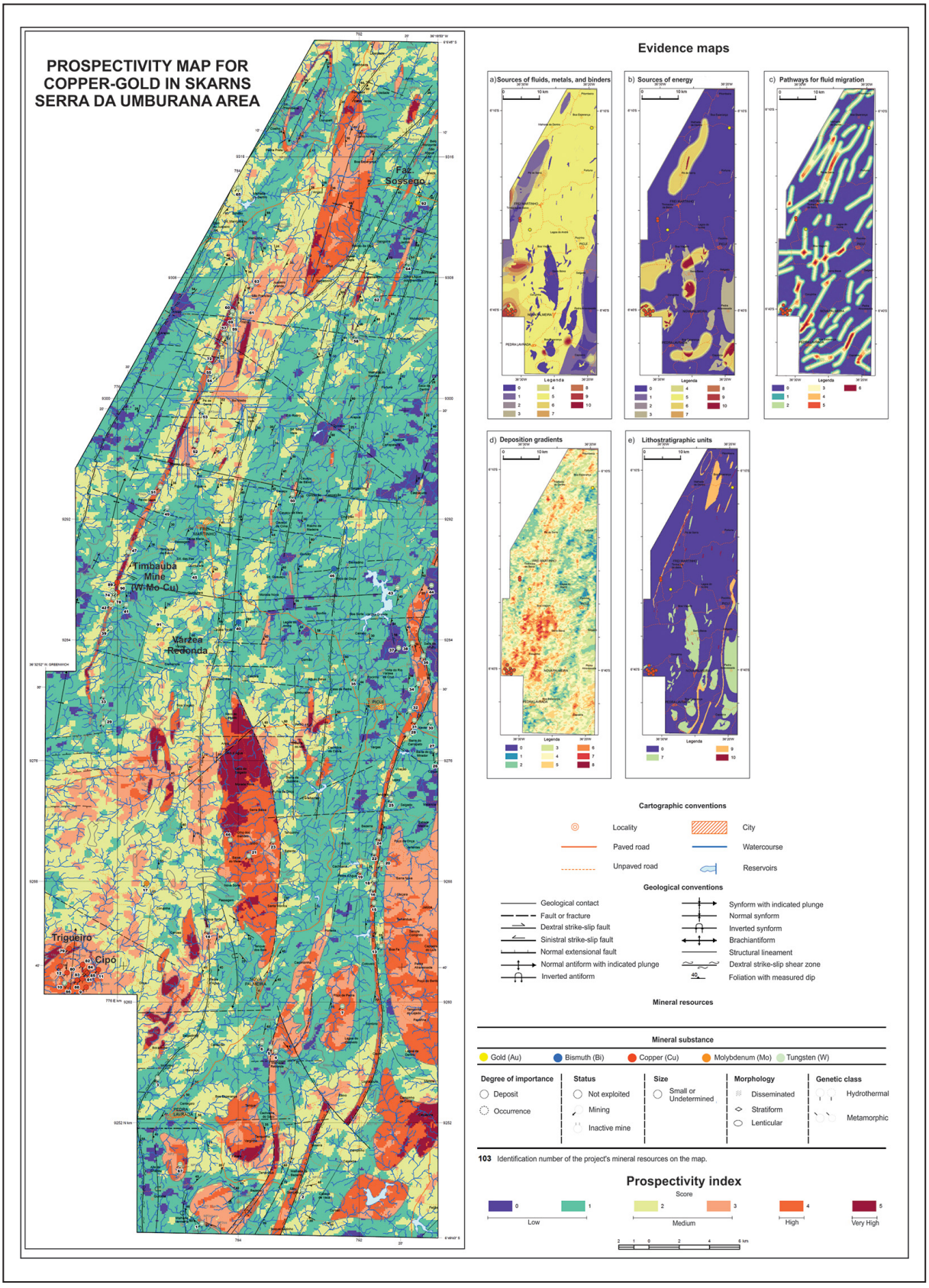

Figure 12: Simplified prospectivity map with its evidence maps for Cu and Au in the Serra da Umburana area (Adapted from Costa et al. 2023b).

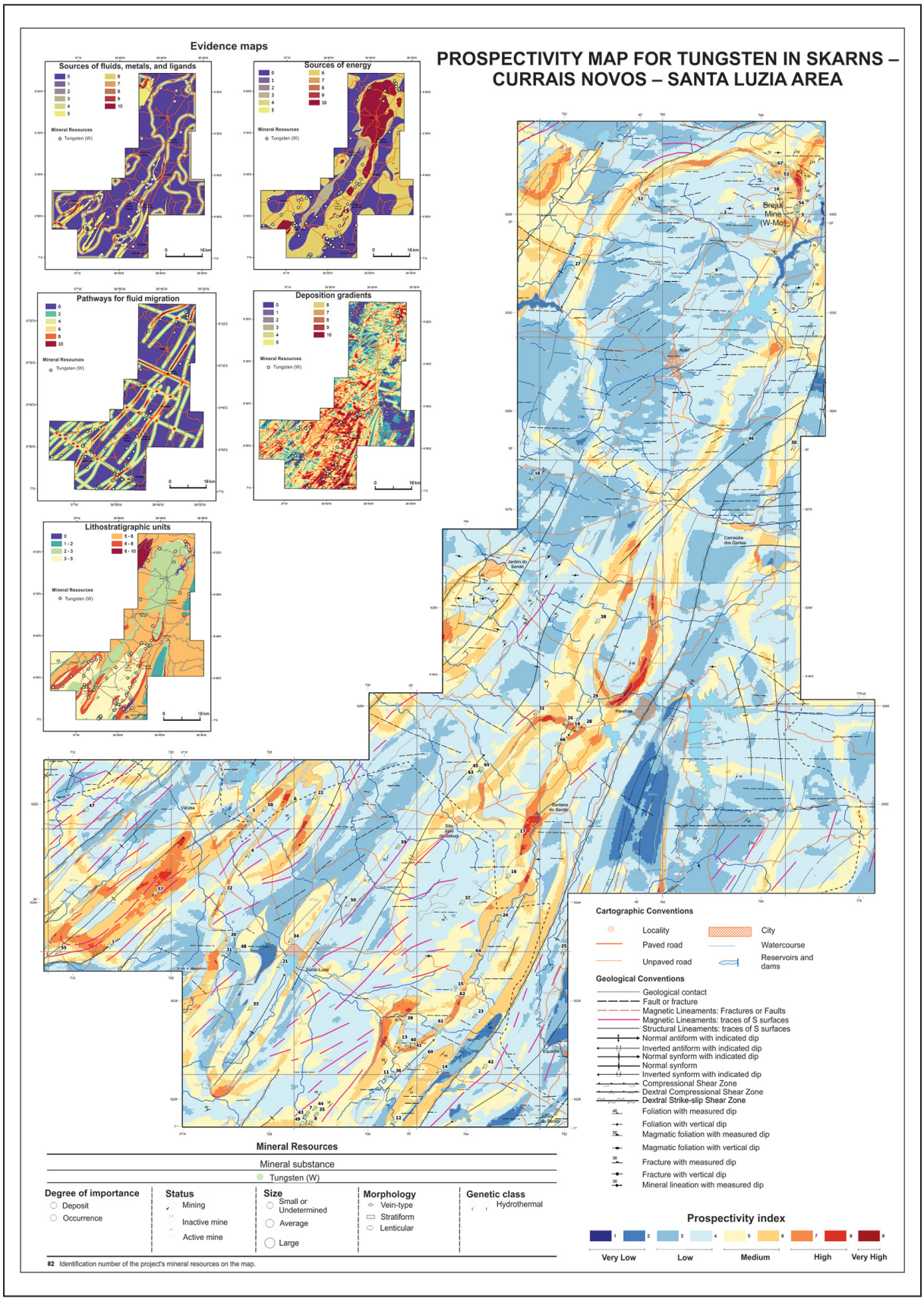

Figure 13: Simplified prospectivity map with its evidence maps for W in the Currais Novos–Santa Luzia area (Adapted from Cavalcante et al. 2025).

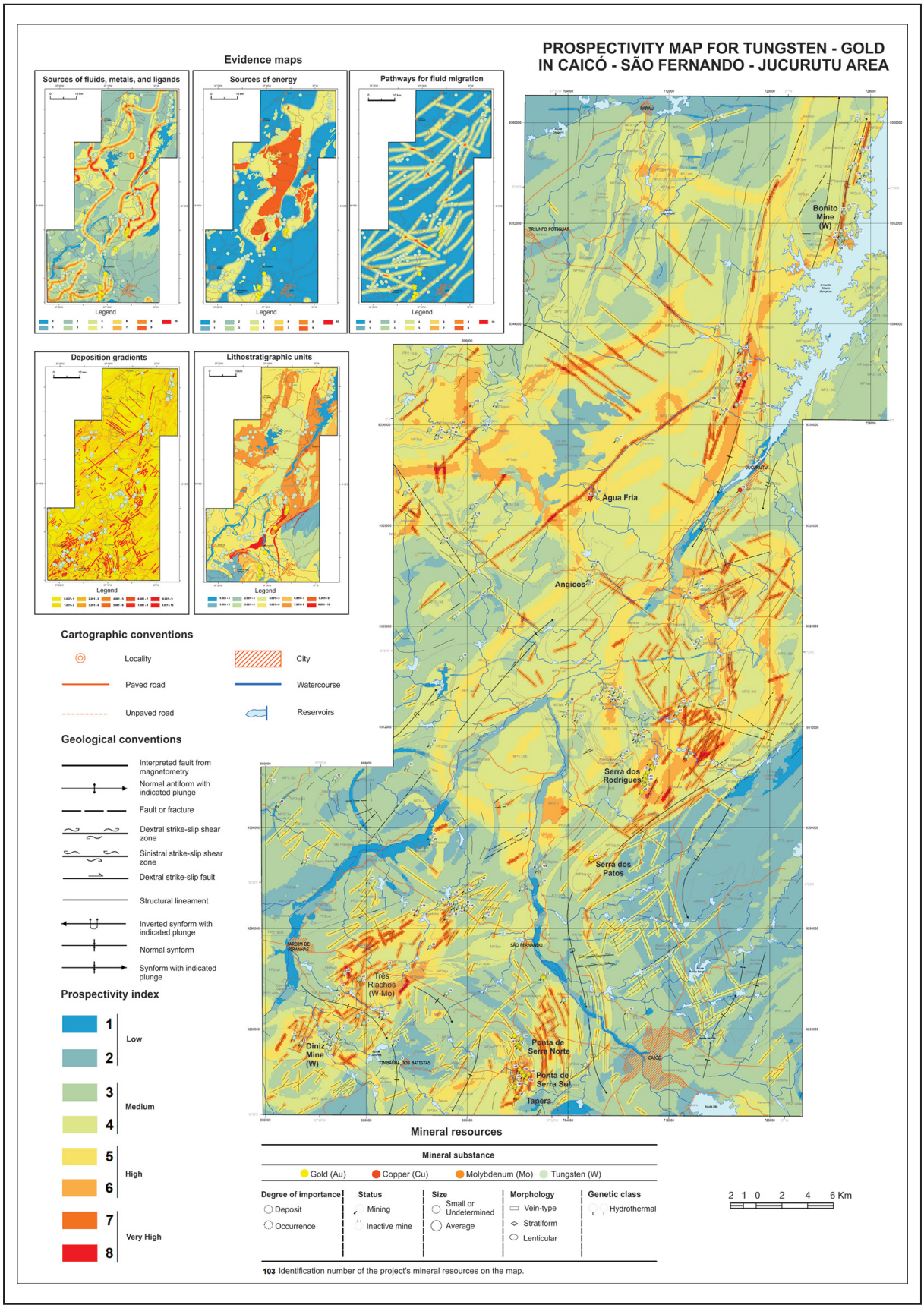

Figure 14: Simplified prospectivity map with its evidence maps for W and Au in the Caicó–São Fernando–Jucurutu area (Adapted from Costa et al. 2024).

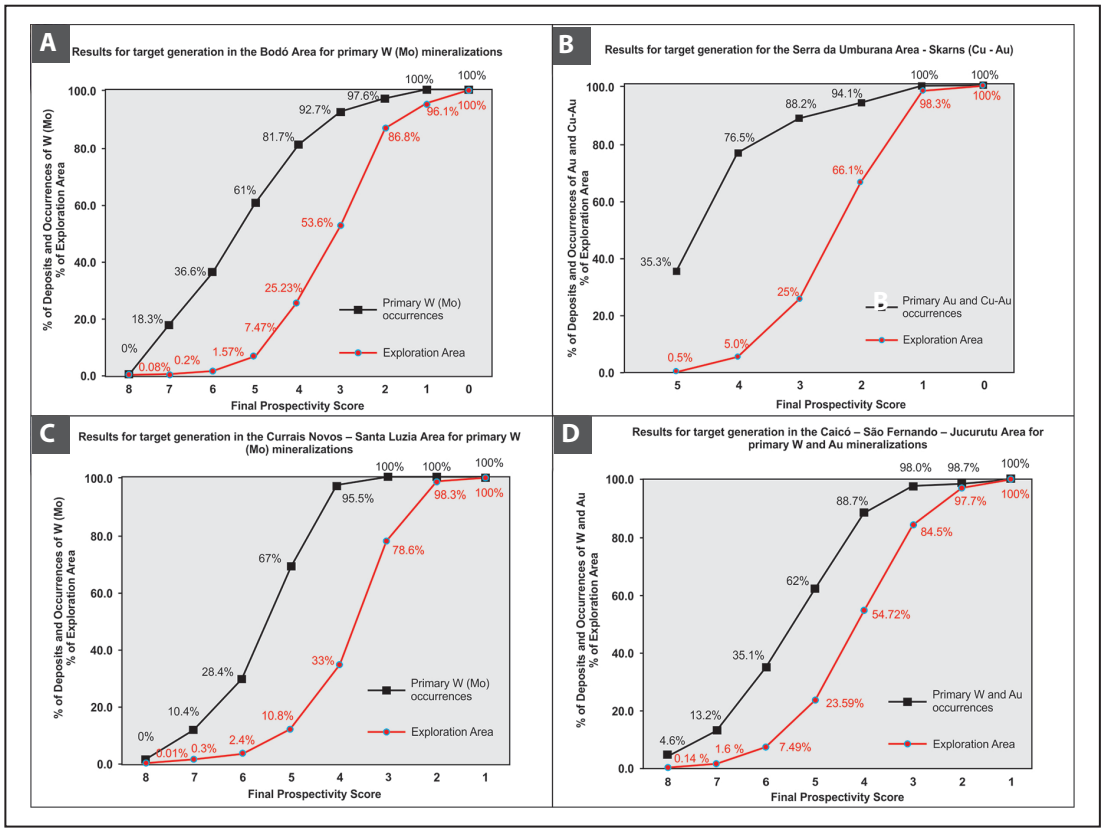

Figure 15: Graphs with the cumulative validation curves of the prospectivity maps for each area. (A) Bodó area, (B) Serra da Umburana area, (C) Currais Novos–Santa Luzia area, and (D) Caicó–São Fernando–Jucurutu area (Adapted from Cavalcante et al. 2024; Costa et al. 2023b; Cavalcante et al. 2025; Costa et al. 2024).

Table 3: Relationship between the prospectivity potential of each area and its prospectivity indices.

Area / Prospectivity Potential	Bodó W-Mo skarn	Serra da Umburana Cu-Au skarn	Currais Novos--Santa Luzia W-Mo skarn	Caicó - São Fernando - Jucurutu W-Au skarns
Very low	--	--	1 to 2	--
Low	0 to 1	0 to 1	3 a 4	1 to 2
Medium: uncertainties in geological processes	2 to 3	2 to 3	5 to 6	3 to 4
High: favorable geological conditions	4 to 5	4	7 to 8	5 to 6
Very high: activity of geological processes relevant to mineralization	6 to 7	5	9	7 to 8

terrestrial gravimetric data and field descriptions, as well as the presence of deep and shallow magnetic lineaments that would act as conduits for the circulation and migration of hydrothermal fluids.

In the crystalline basement, W and Au mineralizations show characteristics of hydrothermal events correlated with Cambrian processes (between 541 and 491 Ma), which occasionally exhibit overprint features, such as the presence of copper sulfides with low Au content filling fractures in the Diniz deposit. Their correlation with the Cambrian period is supported by the spatial association of mineralizations with shear zone structures, as described previously, which primarily affect basement rocks and are spatially close to, or even intersected by pegmatite dikes or leucocratic granites, forming zones favorable for the circulation of mineralizing hydrothermal fluids (Figure 17). In the regional literature, Araújo et al. (2005) determined $^{40}Ar/^{39}Ar$ ages in muscovite from shear zones controlling the Ponta da Serra and Fazenda Simpático mineralizations, obtaining ages of 518–520 Ma and 502–505 Ma, respectively. These results corroborate the field observations and the model presented here.

In the Seridó Group metasediments, the control of mineralizations by fold axes, shear zones, faults, and fractures was also widely observed in the field data of this

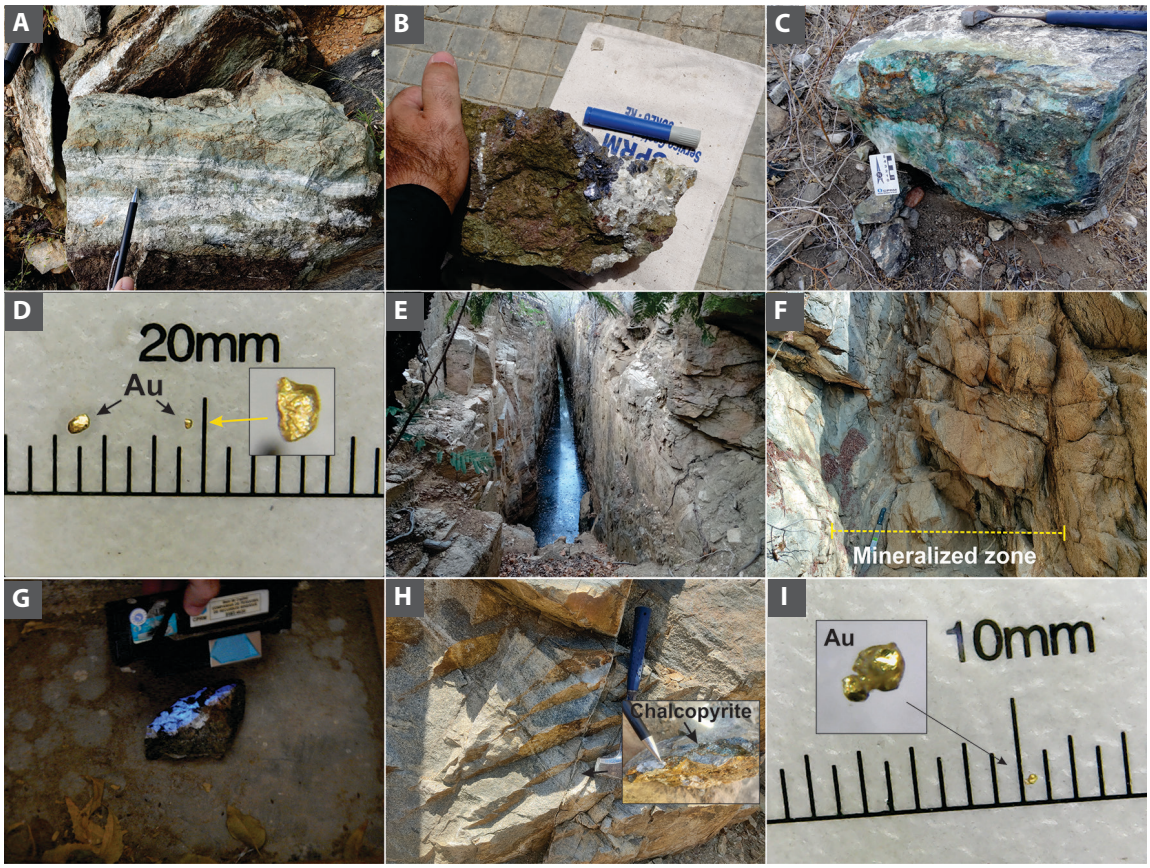

Figure 16: (A) Skarn sample associated with shear zones from the Galo occurrence (Bodó-RN), (B) Skarn sample mineralized with molybdenite from the Brejuí mine (Currais Novos-RN), (C) Amphibolitic skarn sample with quartz veins mineralized in Au and Cu (Sítio Cipó), (D) Au fragments separated from a Au panning concentrate sample from Fazenda Sossego (Currais Novos-RN), (E) Scheelite exploration trench in augen gneiss of the Caicó Complex (Três Riachos, Jardim de Piranhas – RN), (F) Mylonitic rocks in a Au-mineralized shear zone hosted in orthogneiss of the Caicó Complex (Ponta da Serra, Caicó-RN), (G) Skarn samples mineralized in scheelite (crystals with blue fluorescence) from the Diniz Mine gallery (Serra Negra do Norte-RN), (H) Fractures filled with sulfides (chalcopyrite) cutting the orthogneisses in the main quarry of the Diniz Mine (Serra Negra do Norte-RN), and (I) Au grain separated by panning from an ore concentrate sample from the Diniz Mine (Serra Negra do Norte-RN).

Table 4: Lithogeochemical analyses of whole-rock samples collected from the main deposits and artisanal mines in the four mapped areas.

Bodó												
Sample	**Rock**	**As (ppm)**	**Bi (ppm)**	**Te (ppm)**	**Ag (ppm)**	**Cu (ppm)**	**Mo (ppm)**	**Pb (ppm)**	**Zn (ppm)**	**Ba (ppm)**	**W (ppm)**	**Au (ppb)**
RO-R-17B (Cinzas)	Skarn	<1	0.57	<0.05	<0.02	1.2	18.21	13.6	20	<10	2738.8	<5
RO-R-29 (Galo)	Skarn	<1	1.8	<0.05	<0.02	2.5	932.16	17	49	32	58.5	<5
RO-R-33C (Mine Bodó - Pajeú)	Opal	1	12.92	<0.05	<0.02	5.3	275.42	12.1	31	50	>10000	<5
RO-R-33F (Mine Bodó)	Skarn	<1	0.12	<0.05	<0.02	0.5	67.86	2	416	13	5495.5	<5
Serra da Umburana												
AP-R-129B (Cipó)	Amphibolite	<1	3.77	0.23	1.04	4174.3	0.4	6.3	1233	184	4	36
AP-R-129C (Cipó)	Quartz vein	<1	49.83	0.98	12.45	>10000	0.31	1.7	14	42	0.1	1169
AP-R-129D (Cipó)	Amphibolite	<1	22.41	0.28	6.65	8708.6	0.72	13.2	463	309	0.3	686
AP-R-129E (Cipó)	Quartz vein	2	232.33	10.47	67.53	>10000	1	19.6	807	744	0.5	1515
Currais Novos - Santa Luzia												
RO-R-58C (Mine Brejuí)	Skarn	<1	3.73	0.57	1.02	50.1	>10000	1.5	9	<10	86.3	<5
RO-R-58D (Mine Brejuí)	Skarn	<1	2.51	<0.05	0.49	>10000	247.78	9.5	157	119	>10000	<5
RO-R-62C (Mine Brejuí)	Skarn	<1	0.43	<0.05	0.02	44	859.54	8	263	27	>10000	<5

continue

Table 4: Lithogeochemical analyses of whole-rock samples collected from the main deposits and artisanal mines in the four mapped areas. (continued)

Currais Novos - Santa Luzia												
RO-R-63B (Mine Brejuí)	Skarn	<1	63.22	0.06	0.23	37.6	608.86	8	197	50	>10000	<5
RO-R-64A (Mine Brejuí)	Skarn	1	20.7	<0.05	0.03	10.4	261.43	9.5	56	23	>10000	<5
RO-R-64D (Mine Brejuí)	sulfides	<1	3.34	0.54	0.33	1302.3	175.08	2.4	42	21	>10000	<5
Caicó - São Fernando - Jucurutu												
AP-R-20B (S. Rodigues)	Schist	4	0.04	<0.05	0.39	43.7	7.58	18.1	9	522	5.6	1672
AP-R-29A (P. Serra Sul)	Orthogneiss	7	2.18	<0.05	1.59	26.4	0.98	15.6	229	279	1.8	43
AP-R-30C (P. Serra)	Granite	18	0.2	<0.05	0.57	4.6	0.5	43.8	17	352	4.2	11
AP-R-30D (P.Serra)	Pegmatite	21	7.08	0.39	0.5	2.7	0.24	37.5	10	172	3.6	235
AL-R-69A (Serra do Patos)	Schist	2	0.51	1.05	0.4	335.2	3.91	33.3	28	161	1.3	869
AL-R-69B (Serra do Patos)	Schist	<1	0.65	0.23	0.55	1180.3	1.26	27.4	180	538	2.5	1298
AP-R-70A (Mine Diniz)	Skarn	<1	1.73	0.09	0.33	139.8	1.22	16.2	22	79	4.6	31
AP-R-172A (Mine Diniz)	Skarn	<1	20.3	0.16	0.23	7.3	56.31	41.6	74	61	>10000	62
AP-R-172B (Mine Diniz)	Skarn	8	1099	3.37	5.31	684.5	143.44	50.2	85	150	>10000	1013
AP-R-160A (Mine Bonito W)	Skarn	<1	<0.02	<0.05	4.04	2631.6	89.24	25	287	44	7349.9	21
AP-R-160C (Mine Bonito W)	Skarn	<1	<0.02	0.14	1.34	112.1	>10000	39.6	179	<10	91.9	<5
AP-R-162A (Água Fria)	Skarn	2	15.88	1.29	8.61	2156.6	589.36	4.1	964	<10	4985	46
AP-R-163A (Angicos)	Skarn	4	<0.02	0.11	0.06	72.7	423.83	4.8	187	81	3860.1	<5

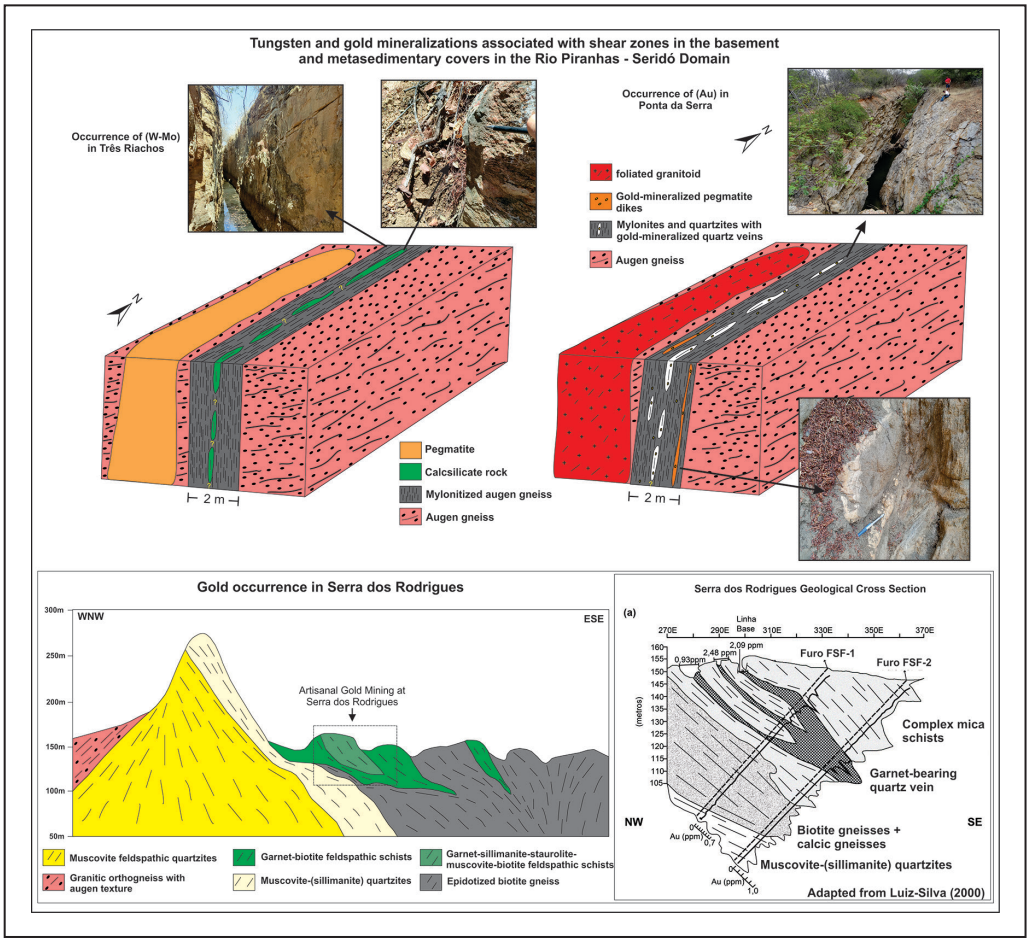

Figure 17: Control model for the main W and Au mineralizations proposed for the Prospectivity Map area of Caicó – São Fernando – Jucurutu (model tungsten and gold mineralizations associated shear zones Adapted from Costa et al. (2024); model from Serra dos Rodrigues compiled and adapted from Luiz-Silva 2000).

study and extensively described in the regional literature (Luiz-Silva 2000; Cavalcanti Neto 2008; Cavalcante et al. 2015; Costa et al. 2023a).

The results obtained in this study show strong coherence with recent discussions in both international and national literature regarding predictive models based on the Mineral Systems framework, as demonstrated by Boadi et al. (2022) in the Ahafo gold district (Ghana) and by Martins et al. (2022) in the Pará Mineral Belt. Across these approaches, a multiepisodic structural architecture emerges as the primary control on the migration and entrapment of mineralizing hydrothermal fluids. In the Seridó region, this pattern is particularly evident in both the crystalline basement and the metasedimentary units of the Seridó Group, where shear zones, faults, folds, and deep lineaments act as preferential pathways for hydrothermal circulation, reproducing the same structural roles documented for the NE–SW and N–NNE fault systems in Ahafo and for the major structural corridors of the Pará Mineral Belt.

Additionally, all studies emphasize the decisive contribution of integrated predictive modeling approaches, particularly those grounded in the Mineral Systems framework. The transformation of geological, structural, geophysical, and geochemical evidence into mappable variables allowed the recognition of regional patterns that often remain obscure when data are analyzed in isolation. In both Ahafo and the Pará Mineral Belt, predictive models successfully reproduced the spatial distribution of known deposits while simultaneously identifying new potential targets in areas lacking previous mineralization records—a behavior identical to that observed in the Caicó–São Fernando–Jucurutu sector of this study.

In the Bodó area (Figure 2), the model assigns greater weight to variables related to the gradient for ore deposition and to lithological units. This choice is justified by the nature of the predominant mineralizations in the region (exoskarns), which present metallogenetic characteristics strongly linked to structural and lithological evidence, such as shallow lineaments, fold axes (both regional and parasitic), and the occurrence of lithostratigraphic units (marbles and calc-silicate rocks) as primary traps for the retention of mineralizing fluids. The high prospectivity index identified in the map, combined with the low spatial distribution values in the “high” and “very high” prospectivity classes, observed in the cumulative curve results, may be related to the good level of prior knowledge regarding the area’s mineral occurrences, as Bodó constitutes one of Brazil’s main W mining districts, widely explored and studied since the 1970s (Torres et al. 1972; Lima et al. 1980). Despite the advances achieved, there is still a need to deepen the understanding of relevant regional structures, such as fold axes and shear zones, as well as possible granitic rocks related to the mineralization sources in the Mina Bodó and Umbuzeiro areas and in the Galo and Isidoro mining sites, which may represent important frontiers for advancing geological and metallogenetic knowledge in the region.

Similar to the Bodó area, the Serra da Umburana area also assigned the greatest weights to the gradients for ore deposition and to lithological units, given the dominance of skarn-type mineralizations in the region. Field observations indicate a strong lithological and structural control over the Au and Cu mineralizations, with clear reflections in the geochemical prospectivity signatures observed in stream sediment samples, as evidenced by the Geochemical Mineralization Prospectivity Index (GPMI). The presence of Cu–Au mineralization associated with bismuth in skarns in the southeastern portion of the Serra da Umburana area may account for the regional anomalies identified in stream-sediment samples from GSB surveys (Costa et al. 2023a).

These skarns, hosted in Neoproterozoic gneisses and schists in the Trigueiro and Saco de Santo Antônio regions (Figure 16C), display a significant spatial distribution and occur near zones of negative gravity anomalies that correlate at the surface with numerous dikes and pegmatite bodies. In this study, such anomalies are interpreted as possible deeper continuations of granitic or pegmatitic intrusions,

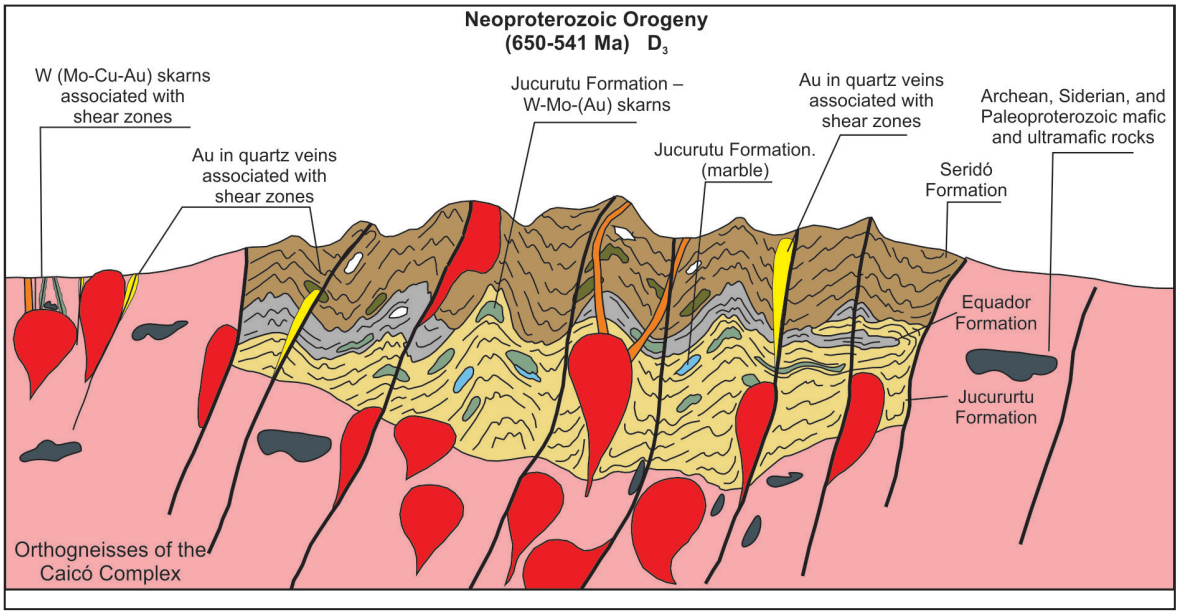

Figure 18: Schematic model for the geotectonic and metallogenetic evolution of the Rio Piranhas – Seridó Domain during the Neoproterozoic orogeny (modified from Costa et al. 2023b).

suggesting that these mineral occurrences represent distal skarns associated with concealed intrusions, whose thermal influence and hydrothermal fluid circulation likely played a key role in the genesis of the Cu–Au–(Bi) systems.

The data presented, together with the occurrences previously reported by Cavalcanti Neto (2008) and Costa et al. (2023a), suggest that the Cu–Au mineralizations hosted in calc-silicate rocks (skarns) and amphibolites of the Jucurutu Formation, in various sectors of the Serra da Umburana area and its surroundings, may represent distal footprints of a larger-scale hydrothermal system. The spatial distribution of these mineralized bodies along basal contacts between schists/paragneisses and quartzites of the Seridó Group, combined with Au grades ranging from 38 to 1500 ppb, indicates the action of mineralizing fluids capable of mobilizing and reconcentrating Au–Cu at different crustal levels. This interpretation aligns with the model proposed by Luiz-Silva (2000) for the São Francisco deposit, in which mass-balance calculations demonstrated that gold is extrinsic to the host rocks and that metals such as Cu and Pb may have been regionally introduced by hydrothermal systems focused along shear zones.

In the model used for the Currais Novos–Santa Luzia area, the greatest weight was assigned to the lithological units variable, followed by fluid sources, metals and ligands, and the gradient for ore deposition. These weights significantly emphasize the importance of the association between mineralizations and host rocks of the skarn type (Jucurutu Formation), as well as their linkage to ductile structures, such as lineaments and, especially, fold hinge zones. Negative Bouguer anomalies related to the presence of exposed or sub-exposed granitic bodies, which most likely act as sources of mineralizing fluids, are also noteworthy. The high and very high prospectivity indices identified in the map are associated with zones having a high density of geological, geochemical, and geophysical data, primarily due to the presence of a large number of mines and mining sites in this area (Boca de Lage, Barra Verde, Saco dos Veados, Olho D'Água, Carnaubinha, Malhada Vermelha, Quixaba, etc.).

In the Caicó–São Fernando–Jucurutu area, regions with high prospectivity index values were identified without records of known mineral occurrences, suggesting potential targets for future exploration and indicating that the area has open prospective potential. Known Au occurrences remain concentrated in the southeastern sector of the area, encompassing the municipalities of Timbaúba dos Batistas (RN), Caicó (RN), and São Fernando (RN), which may indicate possible metallogenetic zoning of the mineral systems or distinct pulses of mineralization, with potential overprinting events. W mineralization strongly controlled by shear zones within crystalline basement rocks raises an important discussion about the role of these structures in the genetic models of local mineralization. Such features may represent either primary mineralizing processes or possible remobilization events, as proposed by Lima et al. (1980), and this constitutes a topic that warrants further detailed investigation.

Additionally, granitic and pegmatitic rocks containing low Au and As concentrations were identified at the Ponta da Serra mining site (Figure 17, Table 4), reinforcing the participation of granitic intrusions in the mineral system of this region, in accordance with the model proposed in Figure 18.

The prospectivity maps generated using the Multiclass Index Overlay (MIO) methodology have as strengths the ability to integrate different types of data — geological, geochemical, geophysical, and structural — into a single product, assigning differentiated weights according to the relevance of each piece of evidence. This flexibility allows both quantitative and qualitative criteria to be incorporated, adjusted through statistical methods (e.g., treatments applied to prospective geochemical data) or prior knowledge, making the model adaptable to different mineral exploration contexts. In addition, the method is easy to implement in GIS environments, allowing rapid updates and reproduction of results, and is particularly useful in areas with limited data, where more complex approaches would be unfeasible. Its methodological transparency also facilitates traceability of decisions and validation by reviewers or technical teams.

On the other hand, the methodology has important limitations, primarily related to the subjectivity in defining weights, which can introduce interpretative bias and compromise the reliability of the final product (Carranza 2009; Yousefi and Carranza 2016). The method does not explicitly address uncertainties or model complex correlations between variables, assuming that all criteria are independent, which rarely occurs in mineral systems. The quality of the results is strongly dependent on the scale and resolution of the input layers, so incompatible or imprecise data can generate significant distortions. Furthermore, the method is sensitive to input errors, meaning that small inaccuracies in the location of structural features, geochemical anomalies, or geological contacts can disproportionately affect the final model response. Therefore, a reliable and consistent database is fundamental for obtaining accurate results.

From a methodological perspective, a clear convergence is observed regarding the advantages and limitations of the Multiclass Index Overlay (MIO) method. As discussed by Boadi et al. (2022) and Martins et al. (2022), the MIO models developed for the Seridó region demonstrated a strong ability to integrate heterogeneous datasets, rapid implementation, and consistent performance in capturing known occurrences relative to the mapped areas. However, they also revealed structural limitations of the method, particularly the subjectivity in weight assignment, the implicit assumption of variable independence, and the strong dependence on the resolution and quality of input layers. These factors contribute to localized variations in model performance, especially in areas with low data density or where key geological features—such as deep intrusions or subtle structural contacts—lack direct expression in the evidential layers. Nevertheless, the internal coherence of the results, reinforced by cumulative curves and by the overlap between high-prospectivity classes and known mineralized zones, confirms the robustness of the models produced and supports the use of MIO as an effective tool in the exploration context of the Seridó region.

The results obtained in this study, the first to integrate multiple datasets across different areas of the PMS at a regional scale, also provide broader insights into the evolution of polymetallic skarn and orogenic gold systems in Neoproterozoic to early Paleozoic orogenic belts. The coexistence of W–Mo–Au–Cu mineralization possibly associated with both exposed and concealed granitic intrusions, combined with the strong structural overprint recorded in the region, reinforces a growing body of global evidence indicating that skarn systems in polydeformed terranes typically develop through multistage magmatic–hydrothermal pulses followed by subsequent structural reactivation.

6. Conclusions

This study demonstrates that the use of predictive maps in mineral exploration can generate significant results for the investigation of areas within provinces with complex geotectonic evolution and metallogeny, as is the case of the Borborema Province. When developed based on well-defined concepts of mineral systems and integrated with consistent sets of geological, geophysical, and geochemical data, these maps have the potential to directly influence the identification of priority areas in regional-scale prospecting surveys. This impact can occur both through the identification of new targets and through the revaluation of previously known areas that were underestimated.

Based on information compiled by the Geological Survey of Brazil (GSB) and available in its database, particularly data generated over the past two decades, as well as the geoscientific knowledge documented in the literature regarding mineral occurrences in the studied areas, this work was able to identify the areas of highest prospectivity in each of the four selected regions. This delimitation was carried out using prospectivity models that consider the presence of W, Au, and their main associated elements, especially Mo and Cu.

The whole-rock lithogeochemical data, integrated with the structural information collected in the field and subsequently interpreted during the data-processing stage, provided key insights into the sources of metals and the processes governing the circulation of mineralizing fluids in the main deposits and mining sites across the region. These integrated datasets significantly strengthened the genetic interpretations proposed in this study and underscored the importance of combining geochemical and structural approaches in regional-scale mineral exploration frameworks.

The results presented reinforce the importance of integrating geoscientific data through modern computational techniques, as evidenced in the analyzed cases. In addition, they highlight the strategic role that regional databases, such as those developed by the GSB, play in advancing mineral research in Brazil.

As a practical outcome of publishing these products, it is expected that their application will help attract and optimize investments in mineral exploration in the Borborema Province, particularly in light of the current increase in global demand for the analyzed mineral commodities.

Finally, it is recommended that future studies further develop integrated modeling by incorporating new data, aiming to improve the accuracy in identifying and discovering mineralized areas and to strengthen the scientific basis for more targeted exploration efforts.

Acknowledgements

The authors thank the mining companies that granted access to their deposits for sample collection and detailed geological work, which were fundamental for the preparation of this scientific article, as well as the reviewers for their valued contributions.

Authorship credits

Author	A	B	C	D	E	F
APC	■	■	■	■	■	
RC	■	■	■	■	■	
NRRD			■	■	■	
REM			■	■	■	
EDM			■	■	■	
GFS		■				■
MALS					■	
PIFT				■	■	
HCFC		■				

A - Study design/ Conceptualization **B** - Investigation/ Data acquisition
C - Data Interpretation/ Validation **D** - Writing
E - Review/Editing **F** - Supervision/Project administration

References

Almeida F.F.M., Hasuy Y., Brito Neves B.B., Fuck R.A. 1981. Brazilian structural provinces: an introduction. Earth Science Reviews, 17(1-2), 1–29. https://doi.org/10.1016/0012-8252(81)90003-9

Almeida R.C., Domingues N.R.R., Cabral Neto I., Fernandes P.R., Oliveira R.G., Silveira F.V., Cunha I.A. 2022. Mapa de favorabilidade para pegmatitos litiníferos na Província da Borborema = Favorability map for lithium pegmatite of the Borborema Pegmatite Province. Recife, SGB, CPRM. Available online at: https://rigeo.sgb.gov.br/handle/doc/23041 / (accessed on 14 January 2026).

Angelim L.A.A., Nesi J.R., Torres H.H.F., Medeiros V.C., Santos C.A., Veiga Junior J.P., Mendes V.A. 2006. Geologia e recursos minerais do estado do Rio Grande do Norte: texto explicativo dos mapas geológico e de recursos minerais do estado do Rio Grande do Norte. Recife, CPRM, FAPERN. Available online at: https://rigeo.sgb.gov.br/handle/doc/10234 / (accessed on 14 January 2026).

Agência Nacional de Mineração (ANM). 2025. SIGMINE - mining cadastre spatial data (shapefile). Available online at: https://geo.anm.gov.br/portal/apps/webappviewer/index.html?id=6a8f5ccc4b6a4c2bba79759aa952d908 / (accessed on 1 September 2025).

Araújo M.N.C., Vasconcelos P.M., Alves da Silva F.C., Jardim de Sá E.F., Sá J.M. 2005. 40Ar/39Ar geochronology of gold mineralization in Brasiliano strike-slip shear zones in the Borborema province, NE Brazil. Journal of South American Earth Sciences, 19(4), 445–460. https://doi.org/10.1016/j.jsames.2005.06.009

Biondi J.C. 2003. Processos metalogenéticos e os depósitos minerais brasileiros. 2nd ed. São Paulo, Oficina de Textos, 552 p.

Boadi B., Sunder Raju P.V., Wemegah D.D. 2022. Analysing multi-index overlay and fuzzy logic models for lode-gold prospectivity mapping in the Ahafo gold district – Southwestern Ghana. Ore Geology Reviews, 148, 105059. https://doi.org/10.1016/j.oregeorev.2022.105059

Brito Neves B.B., Santos E.J., Van Schmus W.R. 2000. Tectonic history of the Borborema province, Northeast Brazil. In: Cordani U.G., Milani E.J., Thomaz Filho A., Campos D.A. (eds.). Tectonic evolution of South America. Rio de Janeiro, 31st International Geological Congress, p. 151–182. Available online at: https://rigeo.sgb.gov.br/handle/doc/19419 / (accessed on 14 January 2026).

Campos L.D., Souza S.M., Sordi D.A., Tavares F.M., Klein E.L., Lopes E.C.S. 2017. Predictive mapping of prospectivity in the Gurupi Orogenic Gold Belt, North–Northeast Brazil: An example of district-scale mineral system approach to exploration targeting. Natural Resources Research, 26, 585–612. https://doi.org/10.1007/s11053-016-9320-5

Carranza E.J.M. 2011. Analysis and mapping of geochemical anomalies using logratio-transformed stream sediment data with censored values. Journal of Geochemical Exploration, 110(2), 167–185. https://doi.org/10.1016/j.gexplo.2011.05.007

Carranza E.J.M. 2009. Geochemical anomaly and mineral prospectivity mapping in GIS. In: Carranza E.J.M. (ed.). Handbook of exploration and environmental geochemistry. Elsevier Science B.V., v. 11, p. III-VIII. https://doi.org/10.1016/S1874-2734(09)70001-4

Carranza E.J.M., Hale M. 2001. Geologically constrained fuzzy mapping of gold mineralization potential, Baguio District,

Philippines. Natural Resources Research, 10, 125–136. https://doi.org/10.1023/A:1011500826411

Cavalcanti Neto J.G. 2008. A faixa cuprífera do Rio Grande do Norte e Paraíba e as relações de contato entre as Formações Equador e Seridó. Holos, 3, 105–118. https://doi.org/10.15628/holos.2008.210

Cavalcante R., Cunha A.L.C., Medeiros V.C. 2015. Mapa do Projeto Províncias Metalogenéticas do Brasil: Área PB–RN (Borborema Leste). 1 mapa, color., 90 × 115 cm, Escala 1:250.000. Available online at: https://rigeo.sgb.gov.br/handle/doc/17659 / (accessed on 14 January 2026).

Cavalcante R., Cunha A.L.C., Oliveira R.G., Medeiros V.C., Dantas A.R., Costa A.P., Lins C.A.C., Larizzatti J.H. 2016. Metalogenia das províncias minerais do Brasil: área Seridó leste, extremo NE da província Borborema (RN–PB). Série Províncias Minerais do Brasil, 8, Brasília, CPRM. Available online at: http://rigeo.sgb.gov.br/handle/doc/17659 / (accessed on 14 January 2026).

Cavalcante R., Medeiros V.C., Costa A.P., Sá J.M., Santos R.V., Rodrigues J.B., Dantas A.R., Nascimento M.A.L., Cunha, A.L.C. 2018. Neoarchean, Rhyacian and Neoproterozoic units of the Saquinho region, eastern Rio Piranhas–Seridó domain, Borborema Province (northeastern Brazil): implications for the stratigraphic model. Journal of the Geological Survey of Brazil, 1(1), 11–29. https://doi.org/10.29396/jgsb.2018.v1.n1.2

Cavalcante R., Costa A.P., Domingos N.R.R., Marques E.D. 2024. Mapa de prospectividade para tungstênio em skarns da área Bodó, Escala 1:100.000. Natal, Serviço Geológico do Brasil. Available online at: https://rigeo.sgb.gov.br/handle/doc/25304 / (accessed on 14 January 2026).

Cavalcante R., Costa A.P., Domingos N.R.R., Marques E.D. 2025. Mapa de prospectividade para tungstênio em skarns da área Currais Novos-Santa Luzia, Escala 1:100.000. Natal, Serviço Geológico do Brasil. Available online at: https://rigeo.sgb.gov.br/handle/doc/25530 / (accessed on 14 January 2026).

Comas-Cufí M., Thió-Henestrosa S. 2011. CoDaPack 2.0: a stand-alone, multi-platform compositional software. In: Egozcue J.J., Tolosana-Delgado R., Ortego M.I. (eds.). CoDaWork'11: International Workshop on Compositional Data Analysis, 4.

Corrêa R.S., Oliveira C. G., Dantas E. L., Botelho N. F. 2019a. Hydrothermal footprint related to regional-scale shear zone-controlled scheelite mineralization, Seridó W-skarn system, northeastern Brazil. Journal of South American Earth Sciences, 103, 102755. https://doi.org/10.1016/j.jsames.2020.102755

Corrêa R.S., Oliveira C. G., Dantas E. L., Della Giustina M.E.S., Hollanda M.H.B.M. 2019b.The root zones of the Seridó W-skarn system, northeastern Brazil: Constraints on the metallogenesis of a large Ediacaran tungsten Province. Ore Geology Reviews, 128, 103884. https://doi.org/10.1016/j.oregeorev.2020.103884

Costa A.P., Dantas A.R. 2018. Geologia e recursos minerais da folha Lajes SB.24-X-D-VI, estado do Rio Grande do Norte. Recife, CPRM – Serviço Geológico do Brasil, 163 p. Available online at: https://rigeo.sgb.gov.br/handle/doc/20238 / (accessed on 14 January 2026).

Costa A.P., Dantas A.R., Cavalcante R., Cunha A.L.C., Spisila A.L., Lima R.B. 2018. Mapa geológico-geofísico: Distrito de Bonfim, SB.24-X-D-VI e SB.24-Z-B-III, Escala 1:50.000. Recife, CPRM – Serviço Geológico do Brasil. Available online at: https://rigeo.sgb.gov.br/handle/doc/18669 / (accessed on 14 January 2026).

Costa A.P., Cavalcante R., Dantas A.R., Cunha A.L.C., Lima, R.B., Spisila, A.L. 2019. Mapa geológico: província mineral do Seridó, Escala 1:350.000. Recife: CPRM. Available online at: https://rigeo.sgb.gov.br/handle/doc/19398 / (accessed on 14 January 2026).

Costa A.P., Cavalcante R., Dantas A.R., Rodrigues J.B., Cunha A.L.C., Lages G.A., Alcântara V.C., Lima R.B., Spisila A.L. 2021. Fragments of juvenile Siderian continental crust in the Rio Piranhas–Seridó Domain, Borborema Province, Northeastern Brazil, as deduced by zircon U–Pb and whole-rock Sm–Nd systematics. Journal of the Geological Survey of Brazil, 4(3), 223–237. https://doi.org/10.29396/jgsb.2021.v4.n3.3

Costa A.P., Cavalcante R., Dantas A.R., Oliveira R.G., Melo S.C., Lages G.A. 2023a. Áreas de relevante interesse mineral (ARIM): evolução crustal e metalogenia da província mineral do Seridó: estados do Rio Grande do Norte e Paraíba. Recife, CPRM. Available online at: https://rigeo.sgb.gov.br/handle/doc/23861 / (accessed on 14 January 2026).

Costa A.P., Domingos N.R.R., Cavalcante R., Meloni R.E., Marques E.D. 2023b. Mapa de prospectividade para cobre-ouro em Skarns - área Serra da Umburana, Escala 1:100.000. Natal, Serviço Geológico do Brasil. Available online at: https://rigeo.sgb.gov.br/handle/doc/24579 / (accessed on 14 January 2026).

Costa A.P., Domingos N.R.R., Cavalcante R., Meloni R.E., Marques E.D. Mapa de prospectividade para tungstênio e ouro: área Caicó - São Fernando – Jucurutu, Escala 1:100.000. Natal, Serviço Geológico do Brasil. Available online at: https://rigeo.sgb.gov.br/handle/doc/25291 / (accessed on 14 January 2026).

CPRM – Serviço Geológico do Brasil. 2010. Projeto aerogeofísico: Paraíba–Rio Grande do Norte e Pernambuco–Paraíba. Programa Geologia do Brasil, Rio de Janeiro, Lasa Engenharia e Prospecções, Prospectors Aerolevantamentos e Sistemas, 389 p. Available online at: https://rigeo.sgb.gov.br/handle/doc/10832 / (accessed on 14 January 2026).

Cunha M.M.B. 2023. Composição química dos minerais-minério e geocronologia Pb-Pb em pirita por LA-ICP-MS da mineralização aurífera do depósito São Francisco, Faixa Seridó, Currais Novos (RN). MSc Dissertation, Universidade Federal de Pernambuco, Recife, 87 p. Available online at: https://repositorio.ufpe.br/handle/123456789/54290 / (accessed on 14 January 2026).

Egozcue J.J., Pawlowsky-Glahn V., Mateu-Figueras G., Barceló-Vidal C. 2003. Isometric logratio transformations for compositional data analysis. Mathematical Geology, 35, 279–300. https://doi.org/10.1023/A:1023818214614

Grunsky E.C. 2010. The interpretation of geochemical survey data. Geochemistry: Exploration, Environment, Analysis, 10(1), 27–74. https://doi.org/10.1144/1467-7873/09-210

Groves D.I. 1993. The crustal continuum model for late Archaean lode-gold deposits of the Yilgarn Block, Western Australia. Mineralium Deposita, 28(6), 366–374. https://doi.org/10.1007/BF02431596

Hagemann S.G., Cassidy K.F. 2000. Archean orogenic lode gold deposits. In: Hagemann S.G., Brown P.E. (eds.). Gold in 2000. Reviews in Economic Geology, 13, 9–68.

Hollanda M.H.B.M., Souza Neto J.A., Archanjo C.J., Stein H., Maia A.C.S. 2017. Age of the granitic magmatism and the W–Mo mineralization in skarns of the Seridó Belt (NE Brazil) based on zircon U–Pb (SHRIMP) and molybdenite Re–Os dating. Journal of South American Earth Sciences, 79, 1–11. https://doi.org/10.1016/j.jsames.2017.07.011

Jardim de Sá E.F. 1994. A Faixa Seridó (Província Borborema, NE do Brasil) e o seu significado geodinâmico na cadeia Brasiliana/Pan-Africana. PhD Thesis, Universidade de Brasília, Instituto de Geociências, Brasília, 803 p.

Jardim de Sá E.F., Kawashita K., Macedo M.H.F., Sá J.M. 1986. Supracrustais monocíclicas no extremo oeste do Rio Grande do Norte. In: Simpósio de Geologia do Nordeste, 12, 62–74.

Kaiser H.F. 1960. The application of electronic computers to factor analysis. Educational and Psychological Measurement, 20(1), 141–151. https://doi.org/10.1177/001316446002000116

Knox-Robinson C.M. Vectorial fuzzy logic: a novel technique for enhanced mineral prospectivity mapping, with reference to the orogenic gold mineralisation potential of the Kalgoorlie Terrane, Western Australia. Australian Journal of Earth Sciences, 47(5), 929-941. https://doi.org/10.1046/j.1440-0952.2000.00816.x

Lapworth D.J., Knights K.V., Key R.M., Johnson C.C., Ayoade E., Adekanmi M.A., Arisekola T.M., Okunlola O.A., Backman B., Eklund M., Everett P.A., Lister R.T., Ridgway J., Watts M.J., Kemp S.J., Pitfield P.E.J. 2012. Geochemical mapping using stream sediments in west-central Nigeria: Implications for environmental studies and mineral exploration in West Africa. Applied Geochemistry, 27(6), 1035–1052. https://doi.org/10.1016/j.apgeochem.2012.02.023

Lima E.A.M., Wanderley A.A., Vieira A.T., Medina A.I.M., Barbosa A.J., Vasconcelos A.M., Amaral C.A., Sato E.Y., Silva E.H.R.O., Leite J.F., Moraes J.F.S., Ribeiro J.A., Nesi J.R., Angelim L.A.A., Calheiros M.E.V. 1980. Projeto Scheelita do Seridó: relatório final. Recife, DNPM, CPRM, 35 v., 1284 p. Available online at: https://rigeo.sgb.gov.br/handle/doc/9240 / (accessed on 15 January 2026).

Lucas D., Hollanda M.H.B.M., Souza Neto J.A., Moraes R., Souza L.C. 2024. Unraveling the evolution of the Bodó W-skarn district in the Seridó Mineral Province (NE-Brazil): constraints from C–O stable isotopes, thermodynamic modeling, and geochronology. Mineralium Deposita, 60, 1-22. https://doi.org/10.1007/s00126-024-01300-4

Luiz-Silva W. 2000. Mineralizações auríferas em veios de quartzo na Faixa Seridó, NE do Brasil: exemplos de depósitos de ouro de fácies anfibolito em faixa móvel proterozóica. PhD Thesis, Universidade Estadual Paulista, Instituto de Geociências e Ciências Exatas, Rio Claro.

Marques E.D., Castro C.C., Barros R.A., Lombello J.C., Marinho M.S., Araújo J.C.S., Santos E.A.M. 2023. Geochemical mapping by stream sediments of the NW portion of Quadrilátero Ferrífero, Brazil:

application of the exploratory data analysis (EDA) and a proposal for generation of new gold targets in Pitangui gold district. Journal of Geochemical Exploration, 250, 107232. https://doi.org/10.1016/j.gexplo.2023.107232

Martins T.F., Seoane J.C.S., Tavares F.M. 2022. Cu–Au exploration target generation in the eastern Carajás Mineral Province using random forest and multi-class index overlay mapping. Journal of South American Earth Sciences, 116, 103790. https://doi.org/10.1016/j.jsames.2022.103790

Medeiros V.C. 2004. Evolução geodinâmica e condicionamento estrutural dos terrenos Piancó Alto Brígida e Alto Pajeú, domínio da Zona Transversal NE do Brasil. PhD Thesis, Universidade Federal do Rio Grande do Norte, Natal, 200 p. Available online at: https://rigeo.sgb.gov.br/handle/doc/105 / (accessed on 15 January 2026).

Medeiros V.C., Cavalcante R., Santos F.G., Rodrigues J.B., Santana J.S., Costa A.P., Cabral Neto I. 2021. The Rio Piranhas–Seridó Domain, Borborema Province, Northeastern Brazil: review of geological geochronological data and implications for stratigraphy and crustal evolution. Journal of the Geological Survey of Brazil, 4(3), 179–207. https://doi.org/10.29396/jgsb.2021.v4.n3.1

Meinert L.D., Dipple G.M., Nicolescu S. 2005. World skarn deposits. In: Hedenquist J.W., Thompson J.F.H., Goldfarb. R.J., Richards. J.P. (eds.). Economic Geology 100th Anniversary Volume, Colorado, Society of Economic Geologists, p. 299-336. https://doi.org/10.5382/AV100.11

Miller H.G., Singh V. 1994. Potential field tilt – a new concept for location of potential field sources. Journal of Applied Geophysics, 32(2-3), 213–217. https://doi.org/10.1016/0926-9851(94)90022-1

Nykänen V., Groves D.I., Ojala V.J., Eilu P., Gardoll S.J. 2008. Reconnaissance-scale conceptual fuzzy-logic prospectivity modelling for iron oxide copper–gold deposits in the northern Fennoscandian Shield Finland. Australian Journal of Earth Sciences, 55(1), 25-38. https://doi.org/10.1080/08120090701581372

Oliveira C.G., Dantas E.L., Souza V.S., Rodrigues Neto L., Dantas R., Silva J.C. 2013. Contribuição ao enquadramento metalogenético da Província Mineral do Seridó. In: Seminário das Províncias Metalogenéticas Brasileiras, 1, 329–366.

Oliveira R.G. 2008. Arcabouço geofísico, isostasia e causas do magmatismo cenozoico da província Borborema e de sua margem continental (Nordeste do Brasil). PhD Thesis, Universidade Federal do Rio Grande do Norte, Natal. Available online at: https://rigeo.sgb.gov.br/handle/doc/270 / (accessed on 15 January 2026).

Pawlowsky-Glahn V., Egozcue J.J. 2016. Spatial analysis of compositional data: a historical review. Journal of Geochemical Exploration, 164, 28–32. https://doi.org/10.1016/j.gexplo.2015.12.010

Pawlowsky-Glahn V., Egozcue J.J., Tolosana-Delgado R. 2015. Modeling and analysis of compositional data. London, John Wiley & Sons, 272 p.

Pereira E.H.R., Botelho N.F., Oliveira C.G., Santos E.V. 2019. Geologia, controle estrutural e mineralogia do escarnito mineralizado em ouro e tungstênio da Mina Bonfim-II, Província Borborema, Rio Grande do Norte, Brasil. Geologia USP, Série Científica, 19(4), 99–120. Available online at: https://ppegeo.igc.usp.br/portal/wp-content/uploads/tainacan-items/13065/49599/13530-18214-1-SM.pdf / (accessed on 15 January 2026).

Reimann C., Filzmoser P., Garrett R. 2002. Factor analysis applied to regional geochemical data: problems and possibilities. Applied Geochemistry, 17(3), 185–206. https://doi.org/10.1016/S0883-2927(01)00066-X

Reimann C., Filzmoser P., Garrett R.G., Dutter R. 2008. Statistical data analysis explained: applied environmental statistics with R. Chichester, John Wiley & Sons, 362 p. https://doi.org/10.1002/9780470987605

Santos F.G., Morais D.M.F., Pinéo T.R.G., Santana J.S., Medeiros V.C. 2023. Updated geological map of the Borborema Province, northeastern Brazil. Journal of the Geological Survey of Brazil, 6(1), 129–133. https://doi.org/10.29396/jgsb.2023.v6.n1.7

Saunders D., Burson K.R., Branch J.F., Thompson C.K. 1993. Relation of thorium-normalized surface and aerial radiometric data to subsurface petroleum accumulations. Geophysics, 58(10), 1417–1427. https://doi.org/10.1190/1.1443357

Silva G.F., Silva A.D.R., Souza Gaia S.M. (orgs.). 2024. An overview of critical and strategic minerals potential of Brazil, 2024 Edition. Brasília, Serviço Geológico do Brasil, 35 p. Available online at: https://rigeo.sgb.gov.br/handle/doc/24748 / (accessed on 16 January 2026).

Souza Neto J.A., Legrand J.M., Volfinger M., Pascal M.-L., Sonnet P. 2008. W–Au skarns in the Neoproterozoic Seridó Mobile Belt, Borborema Province in northeastern Brazil: an overview with emphasis on the Bonfim deposit. Mineralium Deposita, 43(2), 185–205. https://doi.org/10.1007/s00126-007-0155-1

Spector A., Grant F.S. 1970. Statistical models for interpreting aeromagnetic data. Geophysics, 35(2), 293–302. https://doi.org/10.1190/1.1440092

Torres H.H.F., Barbosa A.G., Santos E.J. 1972. Projeto tungstênio – molibdênio: mapeamento geológico da faixa scheelitífera Malhada Limpa – Timbaúba, Rio Grande do Norte e Paraíba. Brasília, CPRM. Available online at: https://rigeo.sgb.gov.br/handle/doc/3345 / (accessed on 16 January 2026).

Trindade I.R. 2000. Estudo geoquímico e geocronológico Rb–Sr e Sm–Nd em zonas de cisalhamento mineralizadas em ouro e suas relações com as rochas encaixantes, e geocronologia Sm–Nd em mineralização de scheelita na Faixa Seridó. MSc Dissertation, Universidade Federal do Rio Grande do Norte, 178 p. Available online at: https://repositorio.ufrn.br/jspui/handle/123456789/18756 / (accessed on 16 January 2026).

Van Schmus W.R., Brito Neves B.B., Williams I.S., Hackspacher P.C., Fetter A.H., Dantas E.L., Babinski M. 2003. The Seridó Group of NE Brazil, a late Neoproterozoic pre- to syn-collisional basin in West Gondwana: insights from SHRIMP U–Pb detrital zircon ages and Sm–Nd crustal residence (TDM) ages. Precambrian Research, 127(4), 287–386. https://doi.org/10.1016/S0301-9268(03)00197-9

Van Schmus W.R. Brito Neves B.B., Hackspacher P.C., Babinski M., Fetter A.H., Dantas E.L. 1997. Application of U–Pb and Sm–Nd geochronology to understanding the geotectonic history of the Borborema Province, NE Brazil and its implications for the evolution of West Gondwana. In: South American Symposium on Isotope Geology, 1, 27–29. Available online at: https://repositorio.usp.br/directbitstream/2548b6d7-cc8e-4e15-bb12-720f3590e37f/950801.pdf / (accessed on 16 January 2026).

Van Schmus W.R., Kozuch M., Brito Neves B.B. 2011. Precambrian history of the Zona Transversal of the Borborema Province, NE Brazil: insights from Sm–Nd and U–Pb geochronology. Journal of South American Earth Sciences, 31(1-2), 227–252. https://doi.org/10.1016/j.jsames.2011.02.010

Yousefi M., Kamkar-Rouhani A., Carranza E.J.M. 2012. Geochemical mineralization probability index (GMPI): a new approach to generate enhanced stream sediment geochemical evidential map for increasing probability of success in mineral potential mapping. Journal of Geochemical Exploration, 115, 24–35. https://doi.org/10.1016/j.gexplo.2012.02.002

Yousefi M., Kamkar-Rouhani A., Carranza E.J.M. 2014. Application of staged factor analysis and logistic function to create a fuzzy stream sediment geochemical evidence layer for mineral prospectivity mapping. Geochemistry: Exploration, Environment, Analysis, 14, 45–58. https://doi.org/10.1144/geochem2012-144

Yousefi M., Carranza E.J.M. 2016. Data-driven index overlay and Boolean logic mineral prospectivity modeling in greenfields exploration. Natural Resources Research, 25(1), 3–18. https://doi.org/10.1007/s11053-014-9261-9